CHAPTER TWO

BACKGROUND AND LITERATURE REVIEW

2.1 Historical Perspective:

The history of fuzzy control applications is very interesting. Since the development of FL theory by Zadeh in 1965[14], its first application to control a dynamic process was reported by Mamdani in 1974[15], and by Mamdani and Assilian in 1975. These were extremely significant contributions because they stirred widespread interest by later workers in the field. Mamdani and Assilian were concerned with the control of a small laboratory steam engine. The control problem was to regulate the engine speed and boiler steam pressure by means of the heat applied to the boiler and the throttle setting of the engine. The process was difficult because it was nonlinear, noisy, and strongly coupled, and no mathematical model was available. The fuzzy control designed purely from the operator's experience by a set of IF... THEN rules was found to perform well and was better than manual control. In 1976, Kickert and Lemke examined the fuzzy control performance of an experimental warm water plant, where the problem was to regulate the temperature of water leaving a tank at a constant flow rate by altering the flow of hot water in a heat exchanger contained in the tank[4][9].

The success of Mamdani and Assilian's work led King and Mamdani (1977) to attempt to control the temperature in a pilot-scale batch chemical reactor by a fuzzy algorithm. Tong (1976) also applied FL to the control of a pressurized tank containing liquid. These results indicated that fuzzy control was very useful for complex processes and gave superior performance over conventional P-l-D control [4].

FL applications in power electronics and motor drives are somewhat recent. Li and Lau (1989) applied FL to a microprocessor-based servo motor controller, assuming a linear power amplifier. They compared the fuzzy-controlled system performance with that of P-l-D control and MRAC and demonstrated the superiority of the fuzzy system. Da Silva et al. (1987) developed a fuzzy adaptive controller and applied it to a

four-quadrant power converter for the first time. Gradually, fuzzy control gathered momentum to other applications in the power electronics and drives areas.
In recent years, fuzzy algorithms have been used to determine R_s .In a research entitled with "A novel stator resistance identification for speed sensorless induction motor drives using observer" , a fuzzy observer, used the motor currents and voltages to estimate $R_{s,}$,was based on a state error dynamic equation of the motor.

Another use for fuzzy control in DTC methods is torque ripple minimization. The torque ripple can be minimized by adjusting the duty cycle based on the torque error signal [16].

More recently, fuzzy controllers have been employed for fault detection. The stator winding fault is the most common fault. The stator currents carry the signature of stator winding faults. A fuzzy algorithm was used to detect stator winding faults in "fuzzy model based on-line stator winding turn fault detection for induction motor", was based on the measured currents [17].

As an alternative to conventional controllers, several fuzzy controller combinations have been introduced to control the torque and flux of induction motor. They, unlike conventional controllers, have the ability to mimic human intelligence by incorporating human experience in a simple way. The variables are described or classified into linguistic terms. Then, the relationship between the linguistic terms of inputs and outputs is described based on the operator's experience as illustrated in, "Application of fuzzy algorithms for control of simple dynamic plant" [15].
Briefly, fuzzy logic has variety of applications applied to induction motors. For instance, it is used for motor control, control enhancement, Fault detection and diagnoses.

2.2 Drive Systems with Induction Motors:

An electric motor driving a mechanical load, directly or through a gearbox or a V-belt transmission, and the associated control equipment such as power converters, switches, relays, sensors, and microprocessors, constitute an *electric drive system.* It

should be stressed that, as of today, most induction motor drives are still basically uncontrolled, the control functions limited to switching the motor on and off. Occasionally, in drive systems with difficult start-up due to a high torque and/or inertia of the load, simple means for reducing the starting current are employed. In applications where the speed, position, or torque must be controlled, ASDs with dc motors are still common. However, ASDs with induction motors have increasing popularity in industrial practice. The progress in control means and methods for these motors, particularly spectacular in the last decade, has resulted in development of several classes of ac ASDs having a clear competitive edge over dc drives[4][7].

Most of the energy consumed in industry by induction motors can be traced to high-powered but relatively unsophisticated machinery such as pumps, fans, blowers, grinders, or compressors. Clearly, there is no need for high dynamic performance of these drives, but speed control can bring significant energy savings in most cases. Consider, for example, a constant-speed blower, whose output is regulated by choking the air flow in a valve. The same valve could be kept fully open at all times (or even disposed of) if the blower were part of an adjustable-speed drive system. At a low air output, the motor would consume less power than that in the uncontrolled case, thanks to the reduced speed and torque [13].

High-performance induction motor drives, such as those for machine tools or elevators, in which the precise torque and position control is a must, are still relatively rare, although many sophisticated control techniques have already reached the stage of practicality. For better driveability, high-performance adjustable-speed drives are also increasingly used in electrical traction and other electric vehicles.

Except for simple two-, three-, or four-speed schemes based on *pole changing,* an induction motor ASD must include a variable-frequency source, the so-called *inverter.* Inverters are dc to ac converters, for which the dc power must be supplied by a *rectifier* fed from the ac power line. The so-called *dc link,* in the form of a capacitor or reactor placed between the rectifier and inverter, gives the rectifier properties of a voltage source or a current source. Because rectifiers draw distorted, nonsinusoidal

currents from the power system, passive or active filters are required at their input to reduce the low-frequency harmonic content in the supply currents.

Inverters, on the other hand, generate high-frequency current noise, which must not be allowed to reach the system. Otherwise, operation of sensitive communication and control equipment could be disturbed by the resultant *electromagnetic interference* (EMI). Thus, effective EMI filters are needed too [13].

For control of ASDs, microcomputers, microcontrollers, and digital signal processors (DSPs) are widely used. When sensors of voltage, current, speed, or position are added, an ASD represents a much more complex and expensive proposition than does an uncontrolled motor. This is one reason why plant managers are so often wary of installing ASDs. On the other hand, the motion-control industry has been developing increasingly efficient, reliable, and user-friendly systems, and in the time to come ASDs with induction motors will certainly gain a substantial share of industrial applications[13].

2.3 Common Loads:

Selection of an induction motor and its control scheme depends on the load. An ASD of a fan will certainly differ from that of a winder in a paper mill, the manufacturing process in the latter case imposing narrow tolerance bands on speed and torque of the motor. Various classifications can be used with respect to loads. In particular, they can be classified with respect to: (a) inertia, (b) torque versus speed characteristic, and (c) control requirements.

High-inertia loads, such as electric vehicles, winders, or centrifuges, are more difficult to accelerate and decelerate than, for instance, a pump or a grinder. The total mass moment of inertia referred to the motor shaft can be computed from the kinetic energy of the drive. Consider, for example, a motor with the rotor inertia of J_M that drives a load with the mass moment of inertia of J_L through a transmission with the gear ratio *of N.* The kinetic energy, E_L, of the load rotating with the angular velocity ω_L is [13]:

$$E_L = \frac{J_L \omega_L^2}{2} \qquad (2\text{-}1)$$

while the kinetic energy, $E_{\mathbf{M}}$, of the rotor whose velocity is ω_M is given by

$$E_{\mathbf{M}} = \frac{J_M \omega_M^2}{2} \tag{2.2}$$

Thus, the total kinetic energy, E_{T}, of the drive can be expressed as

$$E_{\mathrm{T}} = E_{\mathrm{L}} + E_{\mathrm{M}} = \left[\left(\frac{\omega_L}{\omega_M}\right)^2 J_L + J_M\right]\frac{\omega_M^2}{2} = \frac{J_T \omega_M^2}{2} \tag{2.3}$$

where J_{T} denotes the total mass moment of inertia of the system referred to the motor shaft. Because

$$\frac{\omega_L}{\omega_M} = N \tag{2.4}$$

Then

$$J_{\mathrm{T}} = N^2 J_{\mathrm{L}} + J_{\mathrm{M}} \tag{2.5}$$

The difference, T_d, between the torque, T_M, developed in the motor and the *static torque,* T_{L}, with which the load resists the motion is calleda *dynamic torque.* According to Newton's second law,

$$T_{\mathrm{d}} = T_{\mathrm{M}} - T_{\mathrm{L}} = J_{\mathrm{T}} \frac{d\omega_M}{dt} = \frac{J_T}{N} \frac{d\omega_L}{dt} \tag{2.6}$$

or

$$\frac{d\omega_L}{dt} = \frac{NT_d}{J_T} \tag{2.7}$$

Unsurprisingly, the preceding equation indicates that a high mass moment of inertia makes a drive sluggish, so that a high dynamic torque is required for fast acceleration or deceleration of the load.

The concept of an *equivalent wheel* is convenient for calculation of the total mass moment of inertia referred to the shaft of a motor driving an electric vehicle or another linear-motion load. The equivalent wheel is a hypothetical wheel assumed to be directly driven by the motor and whose peripheral velocity, u_L, equals the linear speed of the load. Denoting the radius of the equivalent wheel by r_{eq}, the speed of the load can be expressed in terms of that radius and motor speed as

$$u_{\mathrm{L}} = r_{\mathrm{eq}} \omega_M \tag{2.8}$$

The equation for kinetic energy, E_L, of the load whose mass is denoted by m_L,

$$E_L = \frac{m_L u_L^2}{2} \tag{2.9}$$

can therefore be rearranged to

$$E_L = \frac{m_L (r_{eq} \omega_M)^2}{2} = \frac{J_L \omega_M^2}{2} \tag{2.10}$$

with J_L denoting the effective mass moment of inertia of the load, given by

$$J_L = m_L r_{eq}^2 \tag{2.11}$$

Because the motor is assumed to drive the equivalent wheel directly (i.e, $N = 1$), the total mass moment of inertia, J_T, is equal to the sum of J_T and J_M.

In most loads, the static torque, T_L, depends on the load speed, ω_L .The $T_L(\omega_L)$ relation, usually called a mechanical characteristic, is an important feature of the load, because its intersection with the analogous characteristic of the motor, $T_M(\omega_M)$, determines the steady-state operating point of the drive. Expressing the mechanical characteristic by a general equation

$$T_L = T_{LO} + \tau \omega_L^k \tag{2.12}$$

where T_{LO} and τ are constants, three basic types, illustrated in Figure 1.1, can be distinguished:

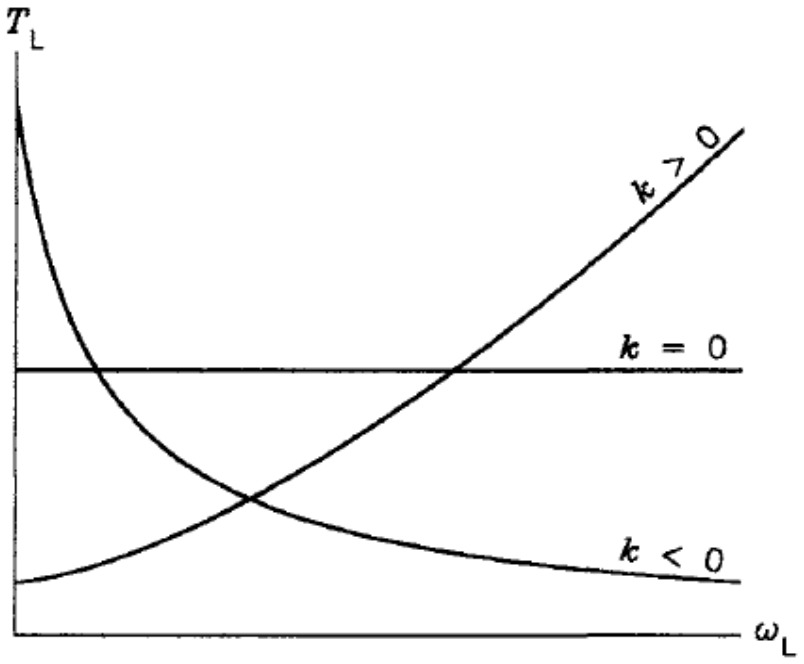

Figure 2.I: Mechanical characteristics of common loads.

1. Constant-torque characteristic, with k ≈0, typical for lifts and conveyors and, generally, for loads whose speed varies in a narrow range only.

2. *Progressive-torque* characteristic, with k > 0, typical for pumps, fans, blowers, compressors, electric vehicles and, generally, for most loads with a widely varying speed.

3. *Regressive-torque* characteristic, with k < 0, typical for winders.

There, with a constant tension and linear speed of the wound tape, an increase in the coil radius is accompanied by a decreasing speed and an increasing torque.

2.4 Operating Quadrants:

The concept of operating quadrants plays an important role in the theory and practice of electric drives. Both the torque, T_M, developed in a motor and speed ω_M, of the rotor can assume two polarities. For instance, watching the motor from the front end, positive polarity can be assigned to the clockwise direction and negative polarity to the counterclockwise direction. Because the output (mechanical) power, P_{out} , of a motor is given by

$$P_{out} = T_M \omega_M \qquad (2.13)$$

the torque and speed polarities determine the direction of flow of power between the motor and load. With $P_{out} > 0$, the motor draws electric power from a supply system and converts it into mechanical power delivered to the load. Conversely, $P_{out} < 0$ indicates a reversed power flow, with the motor being driven by the load that acts as a prime mover. If proper arrangements are made, the motor can then operate as a generator and deliver electric power to the supply system. Such a regenerative mode of operation can be employed for braking a high-inertia load or lowering a load in a lift drive, reducing the net energy consumption by the motor.

The operating quadrants in the already mentioned (ω_M ,T_M) plane correspond to the four possible combinations of polarities of torque and speed, as shown in Figure 2.2. The power flow in the first quadrant and third quadrant is positive, and it is negative in the second and fourth quadrants. To illustrate the idea of operating quadrants, let us consider two drive systems, that of an elevator and that of an electric locomotive. When lifting, the torque and speed of elevator's motor have the same polarity. However, when lowering, the motor rotates in the other direction while the polarity of the torque remains unchanged. Indeed, in both cases the motor torque must counter-balance the unidirectional gravity torque.

Thus, assuming a positive motor speed when lifting, the motor is seen to operate in the first quadrant, while operation in the fourth quadrant occurs when lowering. In the latter situation, it is the weight of the elevator cage that drives the motor, and the potential energy of the cage is converted into electrical energy in the motor. The supply system of the motor must be so designed that this energy is safely dissipated or returned to the power source.

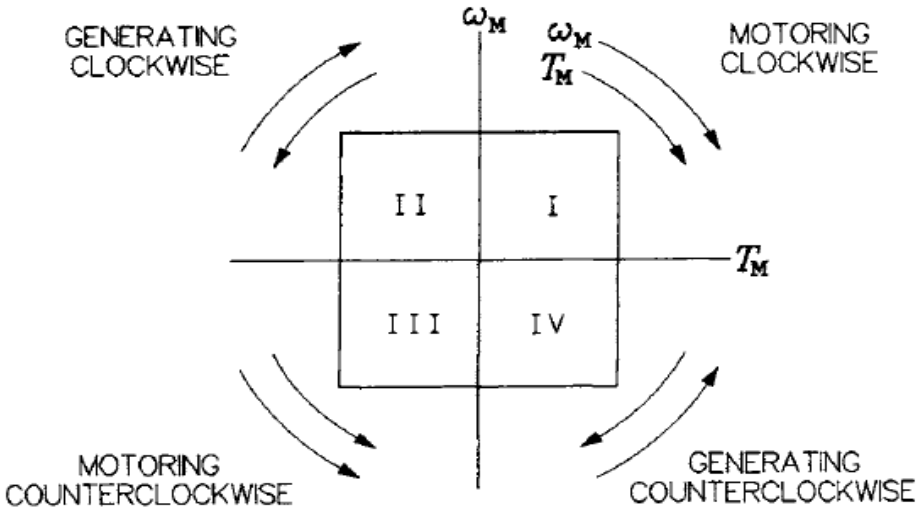

FIGURE 2.2 Operating quadrants in the (ω_M ,T_M) plane.

As for the locomotive, both polarities of the motor speed are possible, depending on the direction of linear motion of the vehicle. Also, the motor torque can assume two polarities, agreeing with the speed when the locomotive is in the driving mode and opposing the speed when braking.

The enormous kinetic energy would strain the mechanical brakes if they were the only source of braking torque. Therefore, all electric locomotives (and other electric vehicles as well) have a provision allowing *electrical braking,* which is performed by forcing the motor to operate as a generator. It can be seen that the two possible polarities of both the torque and speed make up for four quadrants of operation of the drive. For example, first quadrant may correspond to the forward driving, second quadrant to the forward braking, third quadrant to the backward driving, and fourth quadrant to the backward braking. Yet, it is worth mentioning that, apart from electric vehicles, the four-quadrant operation is not very common in practice. Most of the ASDs, as well as uncontrolled motors, operate in the first quadrant only.

Power electronic converters feeding induction motors in ASDs also can operate in up to four quadrants in the current-voltage plane. As known from the theory of electric machines, the developed torque and the armature current are closely related. The same applies to the speed and armature voltage of a machine. Therefore, if a converter-fed motor operates in a certain quadrant, the converter operates in the same quadrant.

2.5 Scalar and Vector Control Methods:

Induction motors can be controlled in many ways. The simplest methods are based on changing the structure of stator winding. Using the so-called *wye-delta switch,* the starting current can easily be reduced. Another type of switch allows emulation of a gear change by the pole changing, that is, changing the number of magnetic poles of the stator. However, in modem ASDs, it is the stator voltage and current that are subject to control. These, in the steady state, are defined by their magnitude and frequency; and if these are the parameters that are adjusted, the control technique belongs in the class of *scalar control* methods. A rapid change in the magnitude or frequency may produce undesirable transient effects, for example a disturbance of the normally constant motor torque. This, fortunately, is not important in low-performance ASDs, such as those of pumps, fans, or blowers. There, typically, the motor speed is open-loop controlled, with no speed sensor required (although current sensors are usually employed in over current protection circuits).

In high-performance drive systems, in which control variables include the torque developed in the motor, *vector control* methods are necessary. The concept of space vectors of motor quantities will be explained later. Here, it is enough to say that a vector represents *instantaneous* values of the corresponding three-phase variables. For instance, the vector of stator current is obtained from the currents in all three phases of the stator and, conversely, all three phase currents can be determined from the current vector. In vector control schemes, space vectors of three-phase motor variables are manipulated according to the control algorithm. Such an approach is primarily designed for maintaining continuity of the torque control during transient states of the drive system.

Needless to say, vector control systems are more complex than those realizing the scalar control. Voltage and current sensors are always used; and, for the highest level of performance of the ASD, speed and position sensors may be necessary as well.

2.6 Construction of Induction Motor:

An induction motor consists of many parts, the stator and rotor being the basic subsystems of the machine. An exploded view of a squirrel-cage motor is shown in Figure 2.3. The motor case (frame), ribbed outside for better cooling, houses the stator core with a three-phase winding placed in slots on the periphery of the core. The stator core is made of thin (0.3 mm to 0.5 mm) soft-iron laminations, which are stacked and screwed together. Individual laminations are covered on both sides with insulating lacquer to reduce eddy-current losses. On the front side, the stator housing is closed by a cover, which also serves as a support for the front bearing of the rotor. Usually,

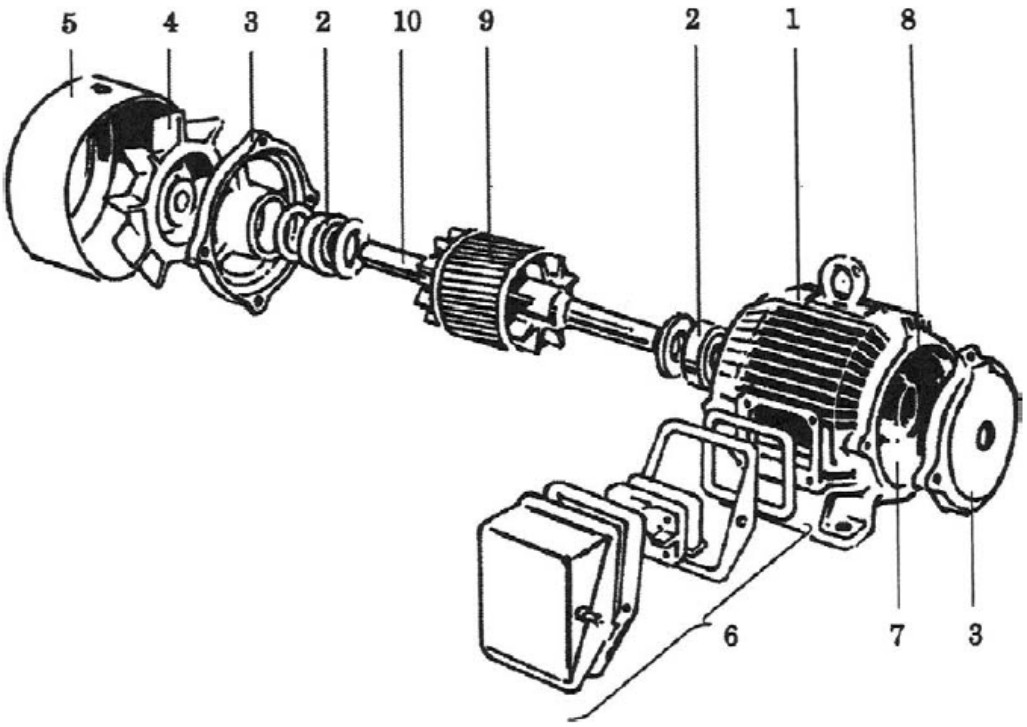

Figure 2.3: Exploded view of an induction motor: (1) motor case (frame), (2) ball bearings, (3) bearing holders, (4) cooling fan, (5) fan housing, (6) connection box, (7) stator core, (8) stator winding (not visible), (9) rotor, (10) rotor shaft.

the cover has drip-proof air intakes to improve cooling. The rotor, whose core is also made of laminations, is built around a shaft, which transmits the mechanical power to the load. The rotor is equipped with cooling fins. At the back, there is another bearing and a cooling fan affixed to the rotor. The fan is enclosed by a fan cover.

Access to the stator winding is provided by stator terminals located in the connection box that covers an opening in the stator housing. *Open-frame, partly enclosed,* and *totally enclosed* motors are distinguished by how well the inside of stator is sealed from the ambient air. Totally enclosed motors can work in extremely harsh environments and in explosive atmospheres, for instance, in deep mines or lumber mills. However, the cooling effectiveness suffers when the motor is tightly sealed, which reduces its power rating.

The squirrel-cage rotor winding, illustrated in Figure 2.4, consists of several bars connected at both ends by end rings. The rotor cage shown is somewhat oversimplified, practical rotor windings being made up of more than few bars (e.g., 23), not necessarily round, and slightly skewed with respect to the longitudinal axis of the motor. In certain machines, in order to change the inductance-to-resistance ratio that strongly influences mechanical characteristics of the motor, rotors with deep-bar cages and double cages are used.

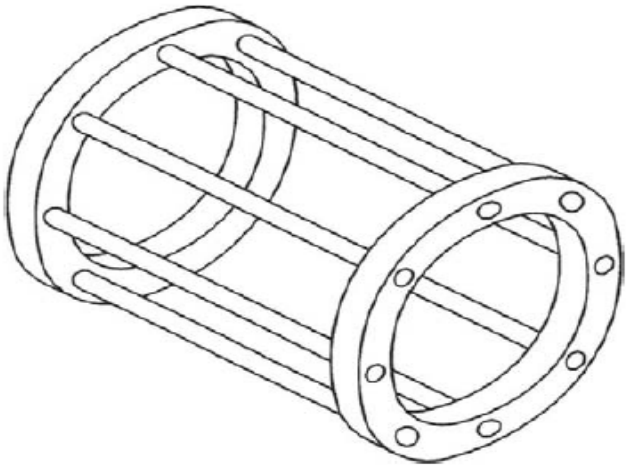

Figure 2.4: Squirrel-cage rotor winding

2.7 Revolving Magnetic Field:

The three-phase stator winding produces a revolving magnetic field, which constitutes an important property of not only induction motors but also synchronous machines. Generation of the revolving magnetic field by stationary phase windings of the stator is explained in Figures 2.5 through 2.10. A simplified arrangement of the windings,

each consisting of a oneloop single-wire coil, is depicted in Figure 2.5 (in real motors, several multiwire loops of each phase winding are placed in slots spread along the inner periphery of the stator). The coils are displaced *in space* by 120° from each other. They can be connected in wye or delta, which in this context is unimportant. Figure 2.6 shows waveforms of currents i_{as}, i_{bs}, and i_{cs} in individual phase windings. The stator currents are given by

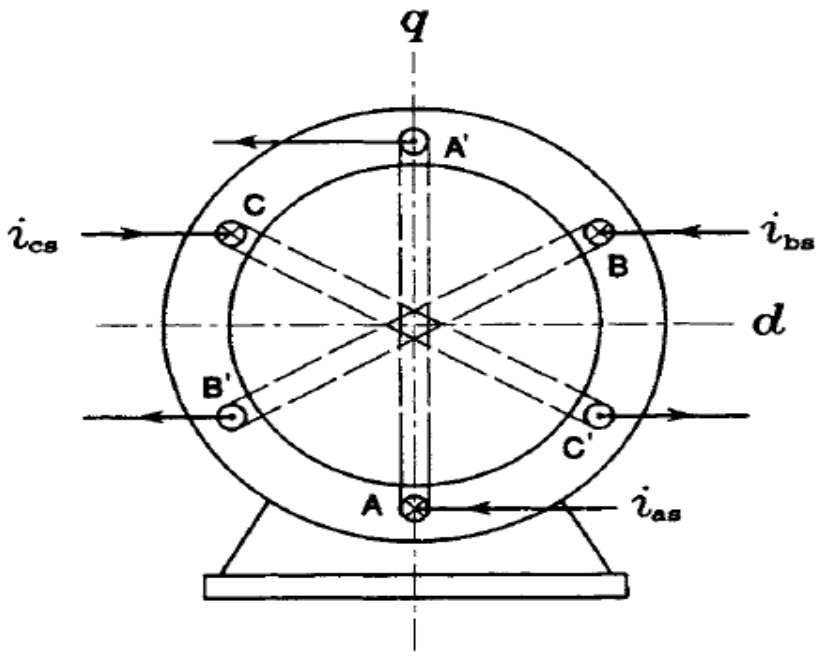

Figure 2.5: Two-pole stator of the induction motor.

$$i_{as} = I_{s,m}\cos(\omega t) \tag{2.14}$$

$$i_{bs} = I_{s,m}\cos(\omega t - \frac{2}{3}\pi),$$

And

$$i_{cs} = I_{s,m}(\omega t - \frac{4}{3}\pi)$$

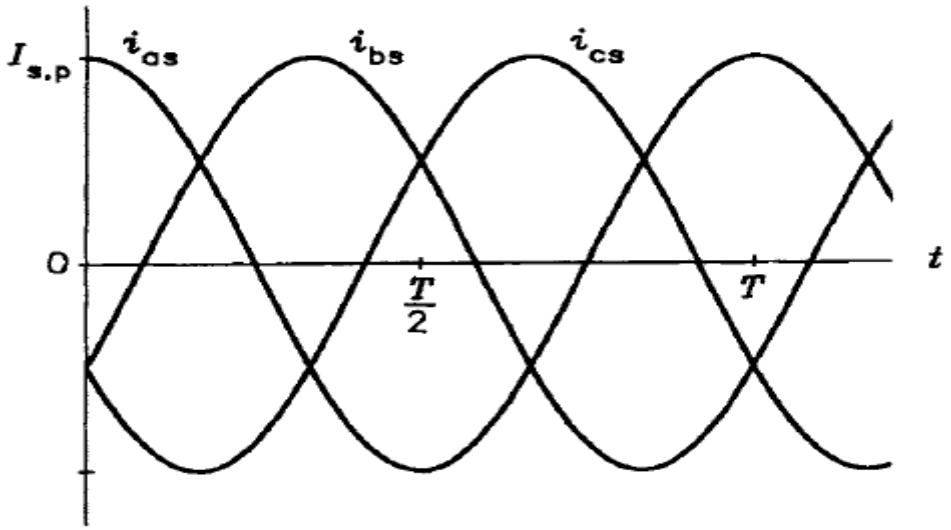

FIGURE 2.6: Waveforms of stator currents.

where $I_{s,p}$ denotes their peak value and ω is the supply radian frequency; they are mutually displaced *in phase* by the same 120°. A phasor diagram of stator currents, at the instant *of t = 0,* is shown in Figure 2.7 with the corresponding distribution of currents in the stator winding. Current entering a given coil at the end designated by an unprimed letter, e.g., A, is considered positive and marked by a cross, while current leaving a coil at that end is marked by a dot and considered negative. Also shown are vectors of the magnetomotive forces (MMFs), $\mathcal{F}_{sa}$, $\mathcal{F}_{sb}$ and $\mathcal{F}_{sc}$ produced by the phase currents. These, when added, yield the vector, $\mathcal{F}_s$, of the total MMF of the stator, whose magnitude is 1.5 times greater than that of the maximum value of phase MMFs. The two half-circular loops represent the pattern of the resultant magnetic field, that is, lines of the magnetic flux, $\boldsymbol{\phi}_s$, of stator.

At $t = T/6$, where T denotes the period of stator voltage, that is, a reciprocal of the supply frequency f, the phasor diagram and distribution of phase currents and MMFs are as seen in Figure 2.8. The voltage phasors have turned counterclockwise by 60°. Although phase MMFs did not change their directions, remaining perpendicular to the corresponding stator coils, the total MMF has turned by the same 60°. In other words, the spacial angular displacement, α, of the stator MMF equals the "electric angle," ω*t*. In general, production of a revolving field requires at least two phase windings displaced *in space,* with currents in these windings displaced *in phase.*

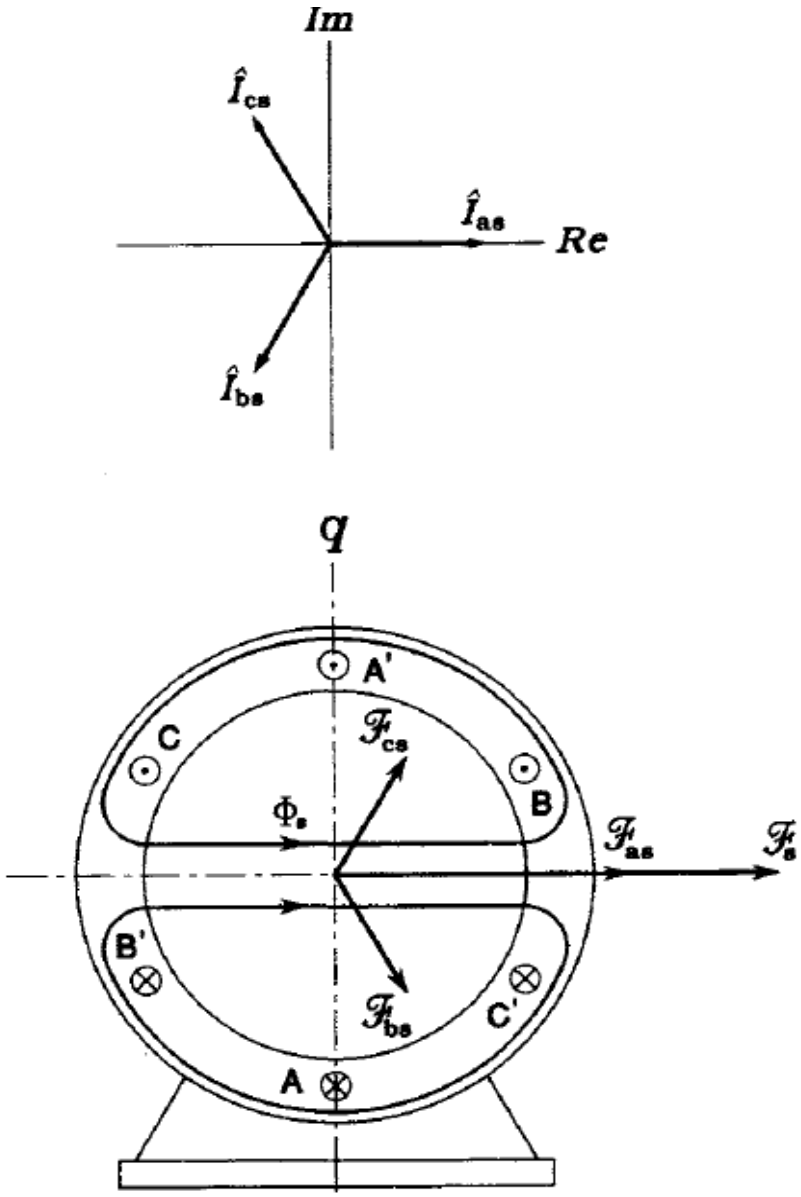

FIGURE 2.7: Phasor diagram of stator currents and the resultant magnetic field in a two-pole motor at $\omega t = 0$.

The stator in Figure 2.5 is called a two-pole stator because the magnetic field, which is generated by the total MMF and which closes through the iron of the stator and rotor, acquires the same shape as that produced by two revolving physical magnetic poles. A four-pole stator is shown in Figure 2.9 with the same values of phase currents as those in Figure 2.6. When, $T/6$ seconds later, the phasor diagram has again turned by 60°, the pattern of crosses and dots marking currents in individual conductors of

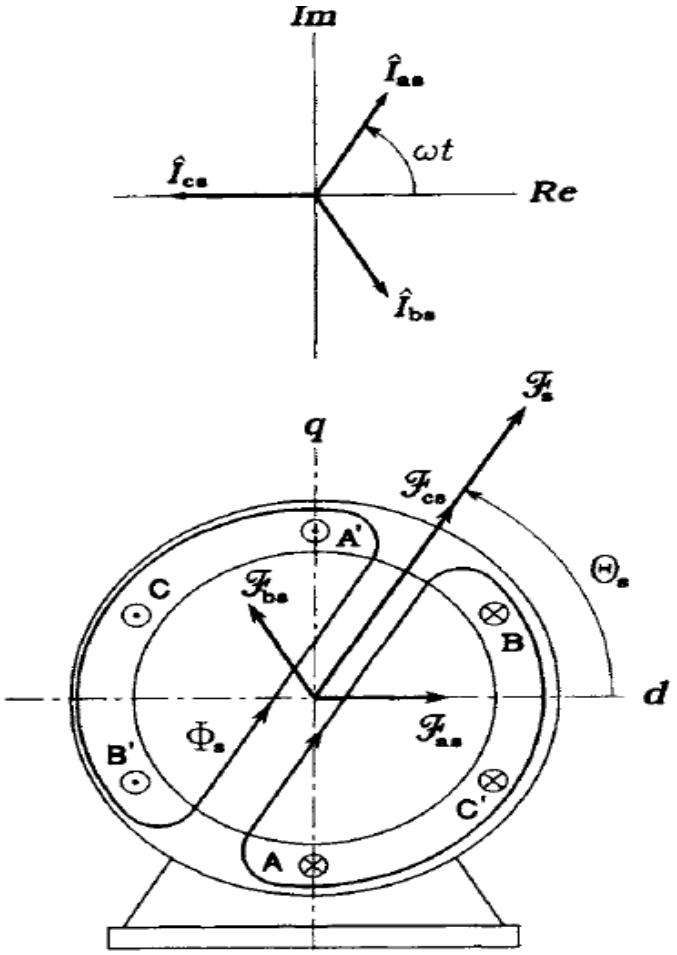

FIGURE 2.8 Phasor diagram of stator currents and the resultant magnetic field in a two-pole motor at $\omega t = 60°$.

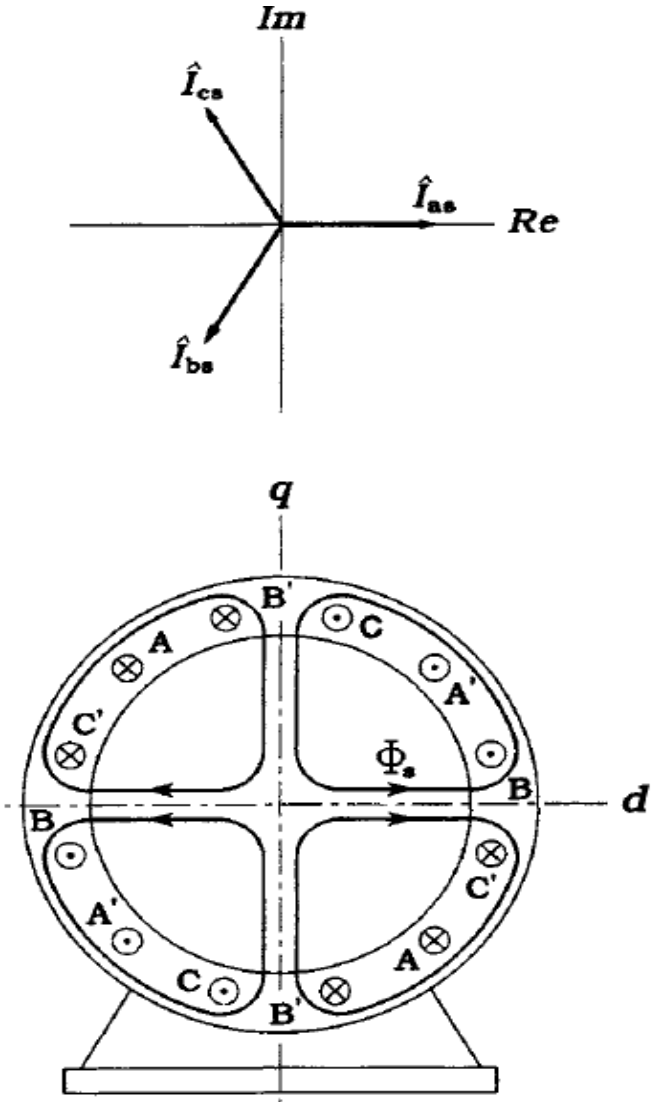

FIGURE 2.9 Phaser diagram of stator currents and the resultant magnetic field in a four-pole motor at $\omega t = 0$.

the stator has turned by 30° only, as seen in Figure 2.10. Clearly, the total MMF has turned by the same spacial angle, α, which is now equal to a half of the electric angle, ωt. The magnetic field is now as if it were generated by four magnetic poles, N-S-N-S, displaced by 90° from each other on the inner periphery of the stator. In general, where p_p denotes the number of pole pairs.

$$\alpha = \frac{\omega t}{P_p} \tag{2.15}$$

Dividing both sides of Eq. (2.15) by *t,* the angular velocity, ω_{syn}, of the field, called a *synchronous velocity,* is obtained as

$$\omega_{syn} = \frac{\omega}{p_P} \tag{2.16}$$

while the *synchronous speed,* ω_{syn}, of the field in revolutions per minute (r/min) is

$$n_{syn} = \frac{60}{p_P} f \tag{2.17}$$

To explain how a torque is developed in the rotor, consider an arrangement depicted in Figure 2.11 and representing an "unfolded" motor.

Conductor CND, a part of the squirrel-cage rotor winding, moves leftward with the speed u_1. The conductor is immersed in a magnetic field produced by stator winding and moving leftward with the speed u_2 , which is greater than u_1. The field is marked by small crossed circles representing lines of magnetic flux, $\boldsymbol{\phi}$ directed toward the page. Thus, with respect to the field, the conductor moves to the right with the speed $u_3 = u_2 - u_1$.

This motion induces (hence the name of the motor) an electromotive force (EMF), *e,* whose polarity is determined by the well-known right-hand rule. Clearly, no EMF would be induced if the speed of the conductor (i.e., that of the rotor) and speed of the field were equal, because according to Faraday's law the EMF is proportional to the rate of change of flux linkage of the conductor. If the conductor was stationary with respect to the field, that is, if the rotor rotated with the synchronous speed, no changes would be experienced in the flux linking the conductor.

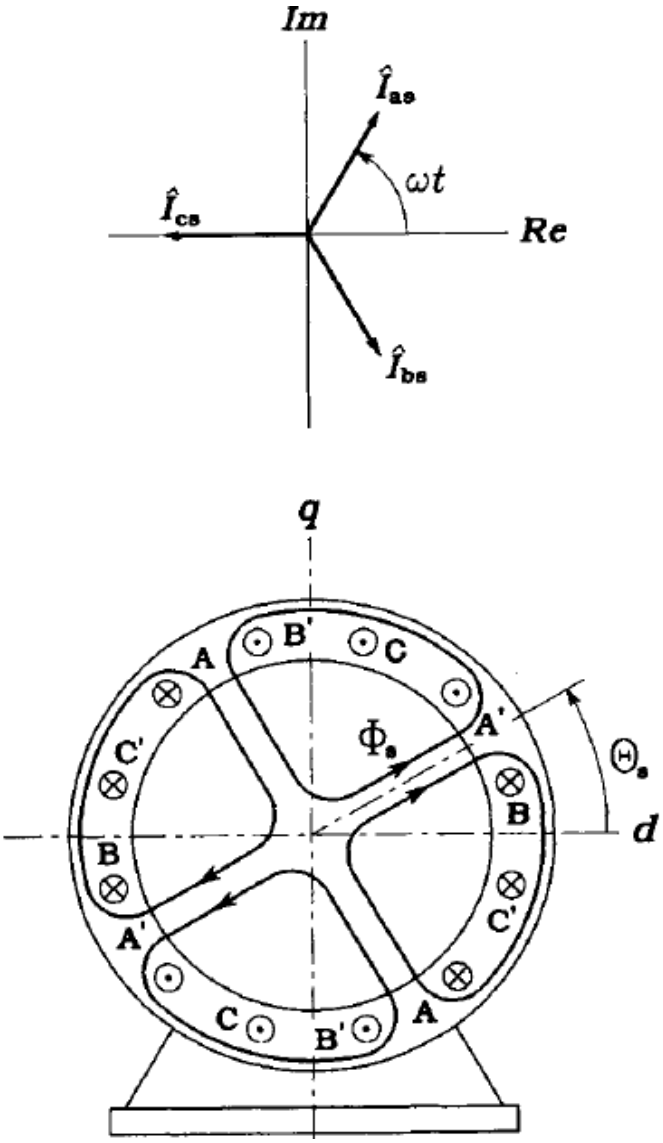

FIGURE 2.10: Phasor diagram of stator currents and the resultant magnetic field in a four-pole motor at ωt = 60°.

The EMF, *e,* produces a current, *i*, in the conductor. The interaction of the current and magnetic field results in an electrodynamic force, *F,*generated in the conductor. The left-hand rule determines direction of the force. It is seen that the force acts on the conductor in the same direction as that of the field motion. In other words, the stator field pulls conductors of the rotor, which, however, move with a lower speed

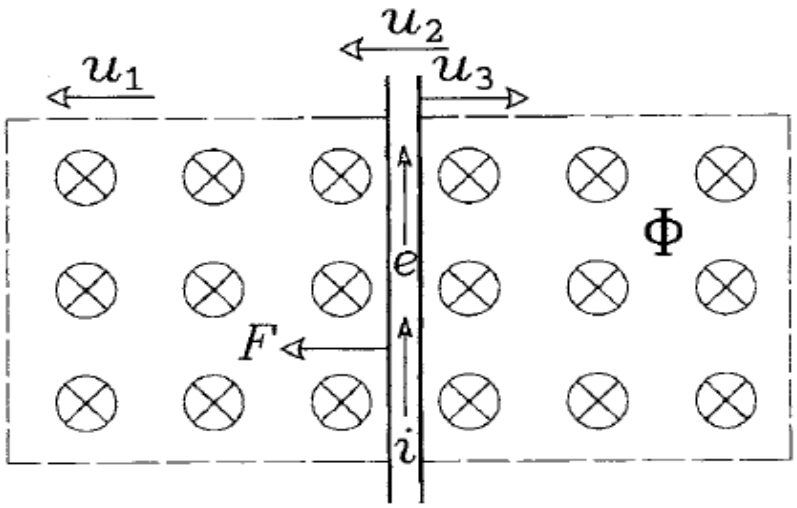

FIGURE 2.11: Generation of electrodynamic force in a rotor bar of the induction motor.

than that of the field. The devel-oped torque, T_M, is a product of the rotor radius and sum of electrodynamic forces generated in individual rotor conductors.

When an induction machine operates as a motor, the rotor speed, ω_M, is less than the synchronous velocity, ω_{syn} . The difference of these velocities, given by

$$\omega_{s1} = \omega_{syn} - \omega_M \tag{2.18}$$

and called a *slip velocity,* is positive. Dividing the slip velocity by ω_{syn} yields the so-called *slip, s,* of the motor, defined as

$$s = \frac{\omega_{s1}}{\omega_{syn}} = 1 - \frac{\omega_M}{\omega_{syn}} \tag{2.19}$$

Here, the slip is positive. However, if the machine is to operate as a generator, in which the developed torque opposes the rotor motion, the slip must be negative, meaning that the rotor must move faster than the field.

2.8 Steady State Equivalent Circuit:

When the rotor is prevented from rotating, the induction motor can be considered to be a three-phase transformer. The iron of the stator and rotor acts as the core, carrying a flux liking the stator and rotor windings, which represent the primary and secondary

windings, respectively. The steady-state equivalent circuit of one phase of such a transformer is shown in Figure 2.12. Individual components of the circuit are:

R_s stator resistance

R_{rr} rotor resistance

X_{ls} stator leakage reactance

X_{lrr} rotor leakage reactance

X_m magnetizing reactance

ITR ideal transformer

The phasor notation based on rms values is used for currents and voltages in the equivalent circuit. Specifically,

$\acute{V}_s$ phasor of stator voltage

$\acute{E}_s$ phasor of stator EMF

$\acute{E_{rr}}$ phasor of rotor EMF

$\acute{I}_s$ phasor of stator current

$\acute{I_{rr}}$ phasor of rotor current

$\acute{I_m}$ phasor of magnetizing current

The frequency of these quantities is the same for the stator and rotor and equal to the supply frequency,f. For formal reasons, it is convenient to assume that both the stator and rotor currents enter the ideal transformer, following a sign convention used in the theory of two-port networks.

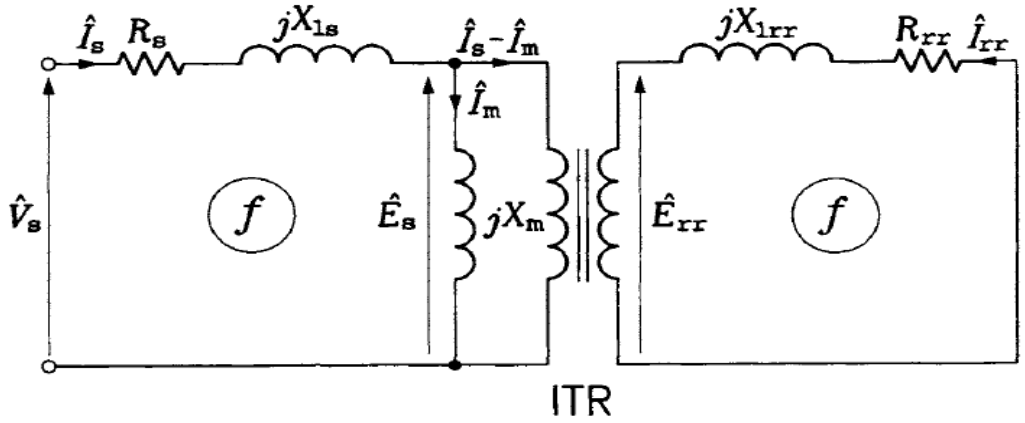

FIGURE 2.12: Steady-state equivalent circuit of one phase of the induction motor at standstill

When the rotor revolves freely, the rotor angular speed is lower than that of the magnetic flux produced in the stator by the slip speed, ω_{sl}. As a result, the frequency of currents generated in rotor conductors is *sf,* and the rotor leakage reactance and induced EMF are sX_{lrr} and sE_{rr} respectively.

The difference in stator and rotor frequencies makes the corresponding equivalent circuit, shown in Figure 2.13, inconvenient for analysis.

This problem can easily be solved using a simple mathematical trick. Notice that the rms value, I_{rr} of rotor current is given by

$$I_{rr} = \frac{sE_{rr}}{\sqrt{R_{rr}^2 + (sX_{lrr})^2}} \tag{2.20}$$

This value will not change when the numerator and denominator of the right-hand side fraction in Eq. (2.20) are divided by *s.* Then,

$$I_{rr} = \frac{E_{rr}}{\sqrt{\left(\frac{R_{rr}}{s}\right)^2 + X_{lrr}^2}} \tag{2.21}$$

which describes a rotor equivalent circuit shown in Figure 2.13, in which the frequency of rotor current and rotor EMF is f again. In addition, the rotor quantities can be referred to the stator side of the ideal transformer, which allows elimination of this transformer from the equivalent circuit of the motor. The resultant final version of

the circuit is shown in Figure 2.15, in which $\acute{E}_r$, $\acute{I}_r$, R_r and X_{lr}, denote rotor EMF, current, resistance, and leakage reactance, respectively, all referred to stator.

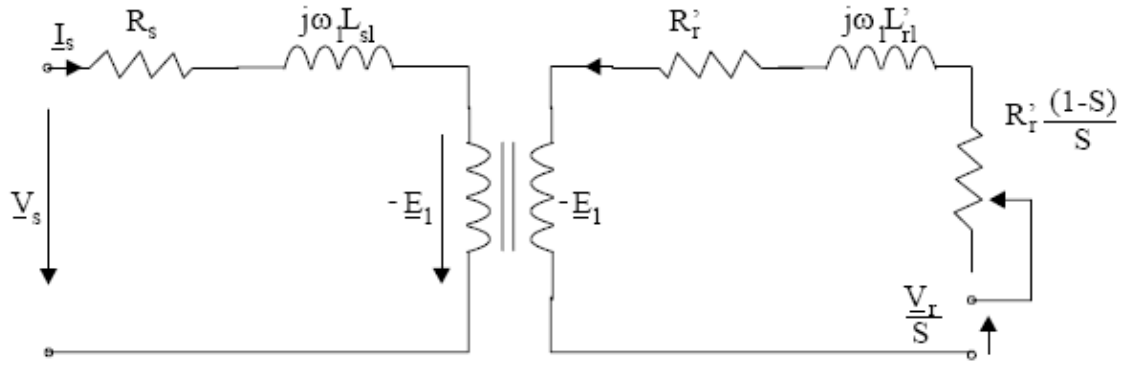

FIGURE 2.13: Per-phase equivalent circuit of a rotating induction motor.

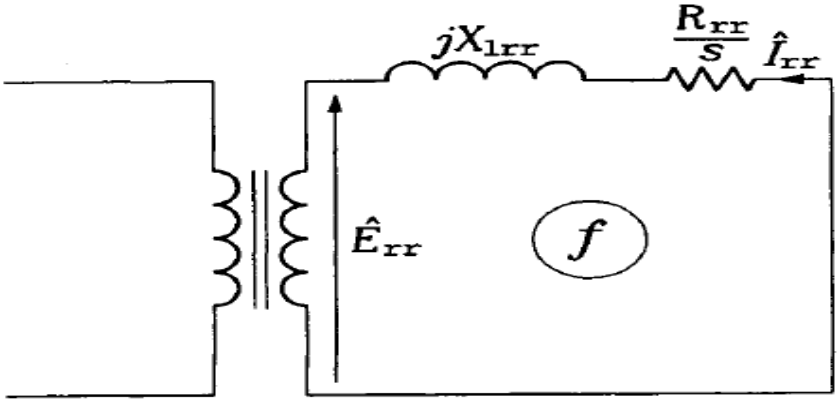

FIGURE 2.14 Transformed rotor part of the per-phase equivalent circuit of a rotating induction motor.

In addition to the voltage and current phasors, time derivatives of magnetic flux phasors are also shown in the equivalent circuit in Figure 2.14. They are obtained by multiplying a given flux phasor by jω. Generally, three fluxes (strictly speaking, flux linkages) can be distinguished: the stator flux, $\hat{A}_s$, airgap flux, $\hat{A}_m$, and rotor flux, $\hat{A}_r$. They differ from each other only by small leakage fluxes. The airgap flux is reduced in comparison with the stator flux by the amount of flux leaking in the stator; and, with respect to the airgap flux, the rotor flux is reduced by the amount of flux leaking in the rotor.

To take into account losses in the iron of the stator and rotor, an extra resistance can be connected in parallel with the magnetizing reactance.

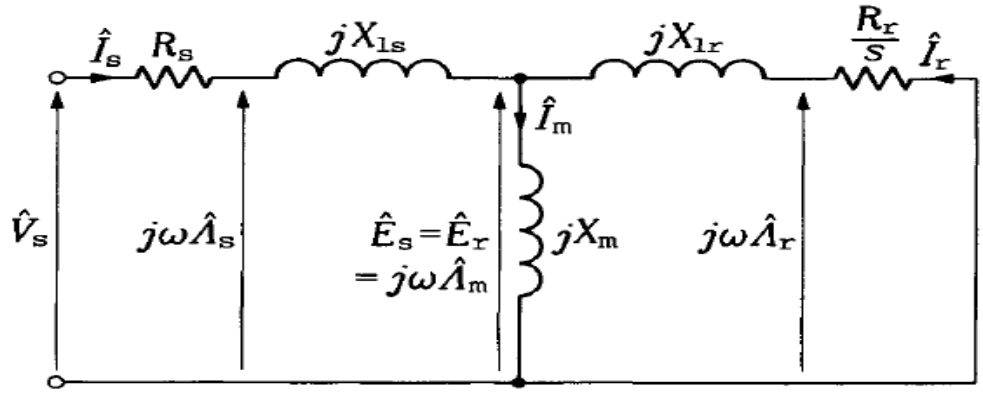

FIG U RE 2.15: Per-phase equivalent circuit of the induction motor with rotor quantities referred to the stator.

Except at high values of the supply frequency, these losses have little impact on dynamic performance of the induction motor. Therefore, throughout the research, the iron losses, as well as the mechanical losses (friction and windage), are neglected.

It must be stressed that the stator voltage, $\acute{V}_s$, and current, $\acute{I}_s$, represent the voltage across a phase winding of stator and the current in this winding, respectively. This means that if the stator windings are connected in wye, $\acute{V}_s$ is taken as the line-to-neutral (phase) voltage phasor and $\acute{I}_s$ as the line current phasor. In case of the delta connection, $\acute{V}_s$ is meant as the line to- line voltage phasor and $\acute{I}_s$ as the phase current.

Although the rotor resistance and leakage reactance referred to stator are theoretical quantities and not real impedances, they can directly be found from simple no-load and blocked-rotor tests.

2.9 Developed Torque:

The steady-state per-phase equivalent circuit in Figure 2.15 allows calculation of the stator current and torque developed in the induction motor under steady-state operating conditions. Balanced voltages and currents in individual phases of the stator winding are assumed, so that from the point of view of total power and torque the equivalent circuit represents one-third of the motor. The average developed torque is given by

$$T_M = \frac{P_{out}}{\omega_M} \qquad (2.22)$$

where P_{out} denotes the output (mechanical) power of the motor, which is the difference between the input power, P_{in}, and power losses, P_{loss}, incurred in the resistances of stator and rotor.

The output power can conveniently be determined from the equivalent circuit using the concept of equivalent load resistance, R_L. Because the ohmic (copper) losses in the rotor part of the circuit occur in the rotor resistance, R_r the R_r/s resistance appearing in this circuit can be split into R_r and

$$R_L = \left(\frac{1}{s} - 1\right)R_r \tag{2.23}$$

as illustrated in Figure 2.16. Clearly, the power consumed in the rotor after subtracting the ohmic losses constitutes the output power transferred to the load. Thus,

$$P_{out} = 3R_L I_r^2 \tag{2.24}$$

And

$$T_M = \frac{3R_L I_r^2}{\omega_M} \tag{2.25}$$

The stator and rotor currents, the latter required for torque calculation using Eq. (2.25), can be determined from the matrix equation

$$\begin{bmatrix} \acute{V}_s \\ 0 \end{bmatrix} = \begin{bmatrix} R_s + jX_s & jX_m \\ jX_m & \frac{R_r}{s} + jX_r \end{bmatrix} \begin{bmatrix} \acute{I}_s \\ \acute{I}_r \end{bmatrix} \tag{2.26}$$

which describes the equivalent circuit in Figure 2.15. Reactances X_s and X_r appearing in the impedance matrix, are called *stator reactance* and *rotor reactance,* respectively, and given by

$$X_s = X_{ls} + X_m \tag{2.27}$$

And

$$X_r = X_{lr} + X_m \tag{2.28}$$

An approximate expression for the developed torque can be obtained from the approximate equivalent circuit of the induction motor, shown in Figure 2.17. Except

for very low supply frequencies, the magnetizing reactance is much higher than the stator resistance and leakage reactance.

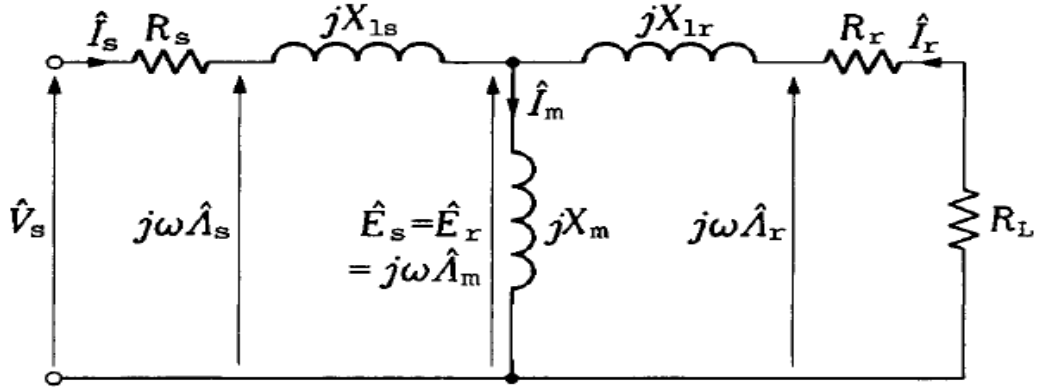

FIG U RE 2.16: Per-phase equivalent circuit of the induction motor showing the equivalent load resistance.

Thus, shifting the magnetizing reactance to the stator terminals of the equivalent circuit does not significantly change distribution of currents in the circuit. Now, the rms value, I_r of rotor current can be calculated as

$$I_r = \frac{V_s}{\sqrt{\left(R_s + \frac{R_r}{s}\right)^2 + X_1^2}} \tag{2.29}$$

Where

$$X_1 = X_{ls} + X_{lr} \tag{2.30}$$

denotes the total leakage reactance. When I_r given by Eq. (2.29), is substi-tuted in Eq. (2.25), after some rearrangements based on Eqs. (2.17) and (2.19), the steady-state torque can be expressed as

$$T_M = \frac{1.5}{\pi}\frac{P_p}{f} V_s^2 \frac{\frac{R_r}{s}}{\left(R_s + \frac{R_r}{s}\right)^2 + X_1^2} \tag{2.31}$$

The quadratic relation between the stator voltage and developed torque is the only serious weakness of induction motors. Voltage sags in power lines, quite a common occurrence, may cause such reduction in the torque that the motor stalls. The torque-slip relation (2.31) is illustrated in Figure 2.18 for various values of the rotor resistance

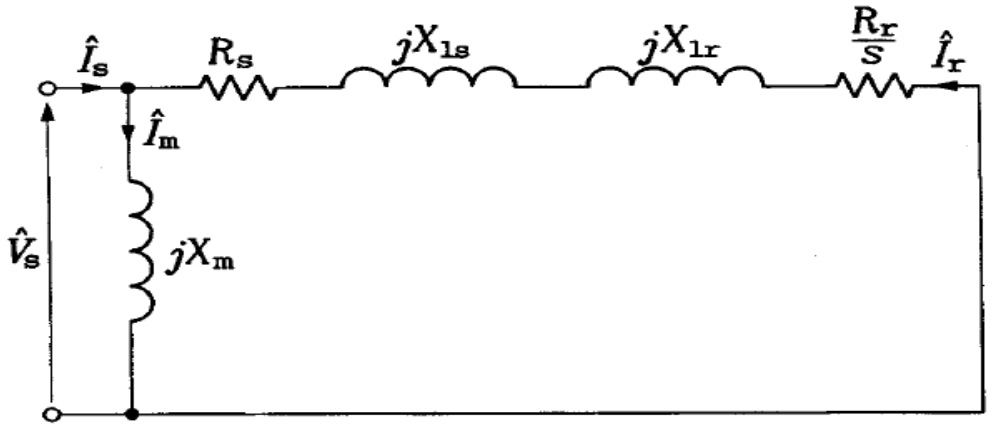

FIGURE 2.17 Approximate per-phase equivalent circuit of the induction motor.

, R_r (in squirrel-cage motors, selection of the rotor resistance occurs in the design stage, while the wound-rotor machines allow adjustment of the effective rotor resistance by connecting external rheostats to the rotor winding). Generally, low values of R_r . are typical for high-efficiency motors whose mechanical characteristic, that is the torque-speed relation, in the vicinity of rated speed is "stiff," meaning a weak dependence of the speed on the load torque. On the other hand, motors with a high rotor resistance have a higher zero-speed torque, that is, the starting torque, which can be necessary in certain applications. A formula for the starting torque, $T_{M,st}$ is obtained from Eq. (2.31) by substituting s = 1 , which yields:

.

$$T_{M,st} = \frac{1.5}{\pi} \frac{P_p}{f} V_s^2 \frac{R_r}{(R_s + R_r)^2 + X_1^2} \tag{2.32}$$

The maximum torque, $T_{M,max}$, called a pull-out torque, corresponds to a critical slip, s_{cr} which can be determined by differentiating T_M, with respect to s and equaling the derivative to zero. That gives:

$$s_{cr} = \frac{R_r}{\sqrt{R_s^2 + X_1^2}} \tag{2.33}$$

and

$$T_{M,max} = \frac{0.75}{\pi} \frac{P_p}{f} \frac{V_s^2}{R_s + \sqrt{R_s^2 + X_1^2}} \tag{2.34}$$

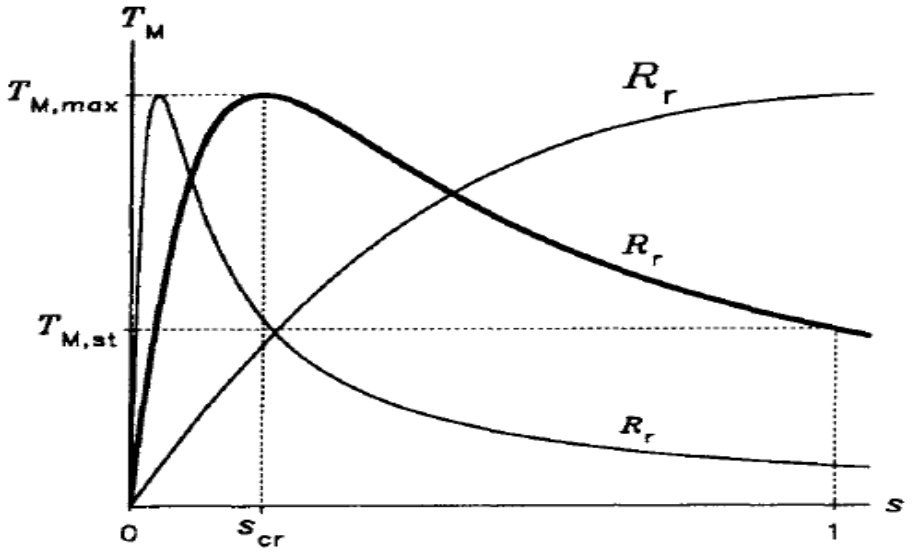

FIGURE 2.18: Torque-slip characteristics of induction motors with various values of the rotor resistance.

It must be reminded that Eqs. (2.29) through (2.34) are based on the approximate equivalent circuit of the induction motor and, as such, they yield only approximate values of the respective quantities.

2.10 Steady State Charactristics:

Based on Eqs. (2.14), (2.17), and (2.23) through (2.27), stator current, torque, input and output power, efficiency, and power factor of an induction motor can easily be computed. The input power, P_{in} efficiency, η, and power factor, PF, can be expressed as:

$$P_{\text{in}} = 3R_{\text{e}}\{\acute{V}_s \acute{I}_s^*\} \tag{2.35}$$

$$\eta = \frac{P_{out}}{P_{in}} \tag{2.36}$$

and

$$PF = \frac{P_{in}}{S_{in}} \tag{2.37}$$

respectively. The apparent input power, S_{in}, in Eq. (2.37) is given by:

$$S_{\text{in}} = 3V_{\text{s}}I_{\text{s}} \tag{2.38}$$

and the P_{in} to S_{in} ratio is equal to the cosine of phase shift between the sinusoidal waveforms of stator voltage and current.

For illustration purposes induction motor, with the rated voltage and frequency, the torque and stator current, input and output power, and efficiency and power factor of this motor are shown in Figures 2.19 through 2.21, respectively. All these variables are plotted as functions of the r/min speed, *n.* The latter is related to the angular velocity, ω_M, of the motor, expressed in rad/s, as

$$n = \frac{30}{\pi}\,\omega_M \tag{2.39}$$

The rated speed, $n_{rat;}$ torque, $T_{M,rat}$; current, $I_{s,rat}$; and power, P_{rat} are marked by a broken line to highlight the rated conditions of the motor.

The rated torque, current, and powers are much lower than their maximum values.

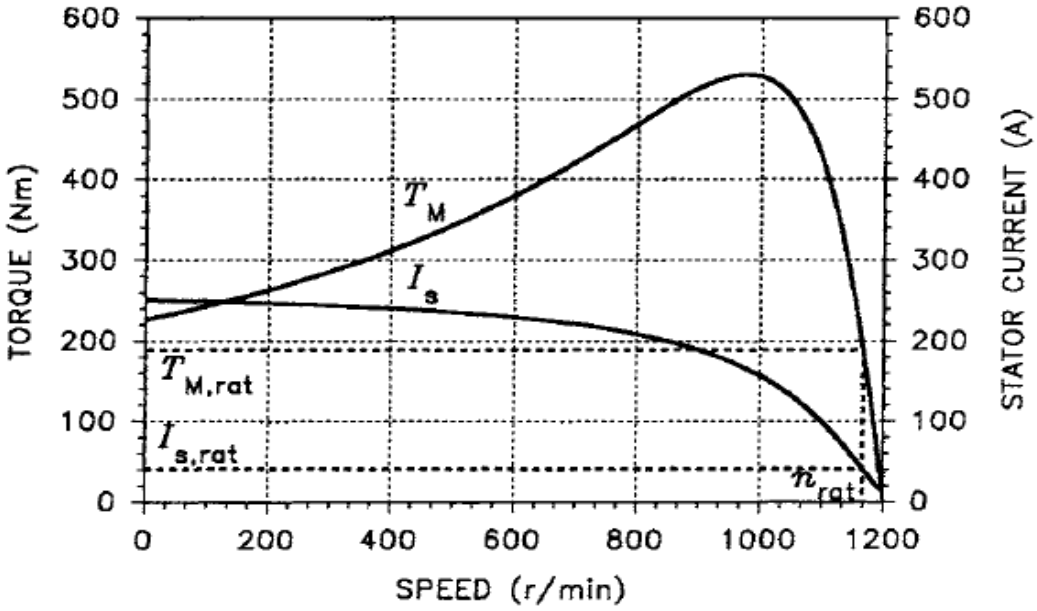

FIGURE 2.19: Stater current and developed torque versus speed

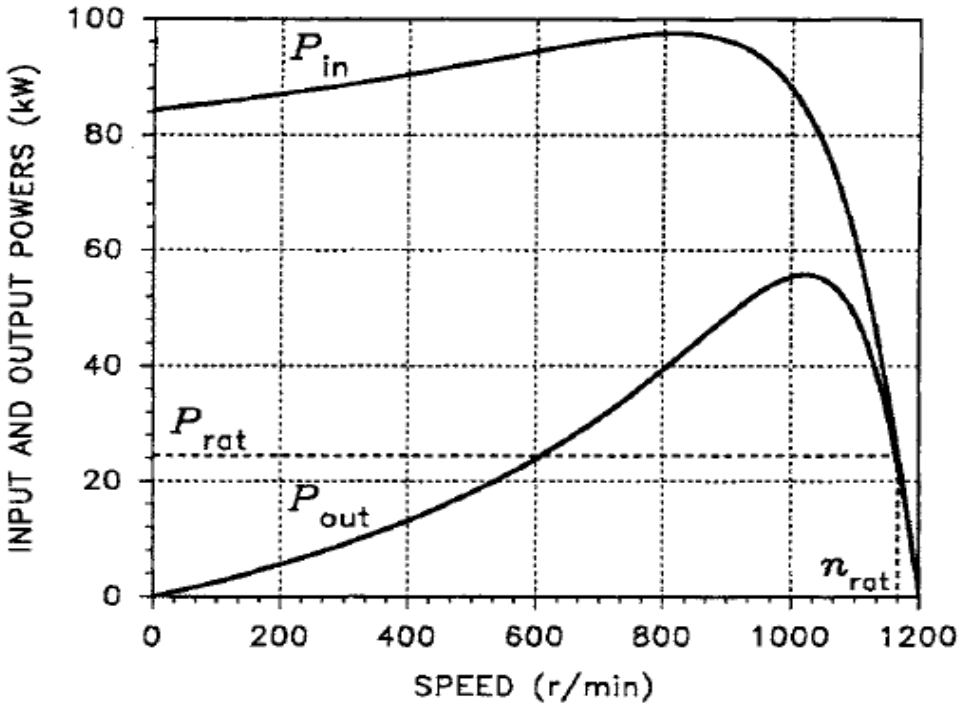

FIGURE 2.20: Input power and output power versus speed

It must be pointed out that, in the steady state, induction motors operate only on the negative-slope part of the torque curve, that is, below the critical slip. When the load increases, the resultant imbalance of the motor and load torques causes deceleration of the drive system. This results in an increased motor torque that matches that of the load, ensuring stability of the operation. Conversely, when the load decreases, the motor accelerates until the load torque is matched again.

In Figures 2.19 through 2.21, the motor speed is limited to the 0 to n_{syn} range, n_{syn} denoting the synchronous speed in r/min. This can be translated into the 1 to 0 range of slip. However, in general, an induction machine can operate with any value of slip, positive or negative. In Figure 2.21, the torque and stator current versus speed curves, such as those in Figure 2.18, are extended over the speed range from n_{syn} to 2 n_{syn}, so that the slip range is 2 to -1. The negative magnitude, I_s, of the stator current at supersynchronous speeds is meant to indicate that the phase shift of the current with respect to the stator voltage is greater than 90° and less than 270°. This implies a negative real power consumed by the motor, that is, the machine operates as a generator. Figure 2.21 illustrates three possible modes of operation of the induction

motor: (1) *braking,*with $s > 1$(i.e., $n < 0$); (2) *motoring,* with $0 < s < 1$ (i.e., $0 < n < n_{syn}$); and (3) *generating,* with $s < 0$ (i.e., $n > n_{syn}$).

In the braking mode, the rotor is forced to rotate against the stator field, which causes high EMFs and currents induced in the rotor conductors. This mode can easily be imposed on a motor by reversing the field, which is accomplished by interchanging two leads between the power line and stator terminals, that is, by changing the phase sequence. However, the braking torque is low, so that this method of slowing the motor down is not very effective. In addition, both the kinetic energy given up by the load and the electric energy supplied to the motor are dissipated in the rotor winding. Thus, no energy is recovered, and the motor is likely to overheat.

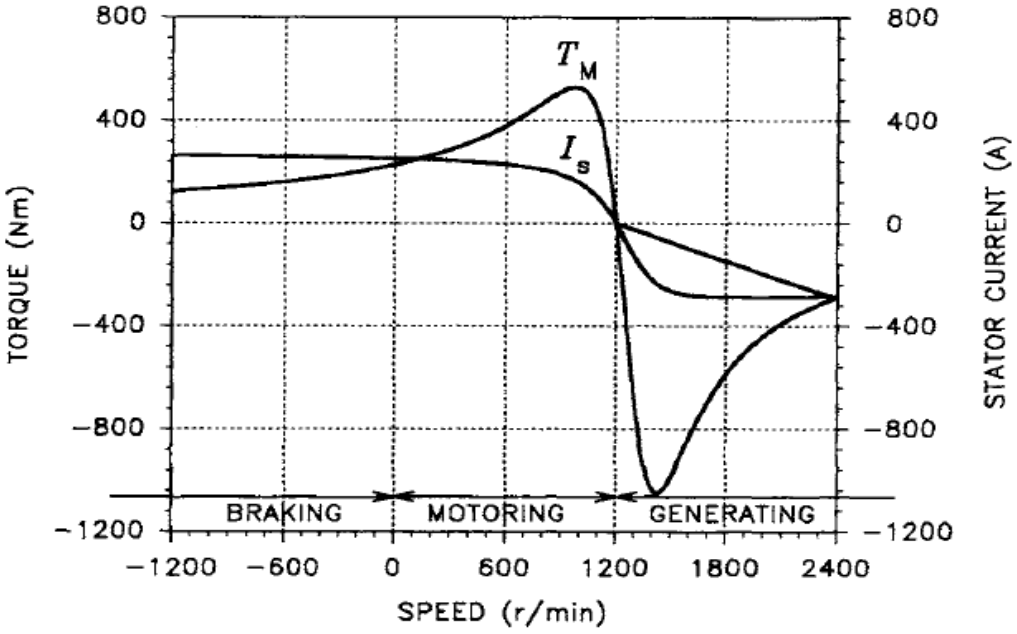

FIGURE 2.21 Torque and current characteristics of the induction motor in a wide speed range.

Much more efficient braking results from forcing the motor to operate in the generating mode, which requires that the rotor turns faster than the field. This is done by reducing the field speed, n_{syn}, so that it revolves slower than the rotor. According to Eq. (2.17), it can be done by increasing the number, P_p, of pole pairs of the stator or by decreasing the supply frequency, f. Indeed, certain motors have stator windings so arranged that they can be connected in more than one configuration, yielding, for instance, $p_p = 1$ and $P_p = 2$. In the adjustable-speed drive systems, the motor is fed

from an inverter, which supplies stator currents of variable frequency. There, the generating mode can easily be enforced by keeping track of the rotor speed and reducing the supply frequency accordingly.

2.11 Fuzzy Logic Principles:

2.11.1 Introduction:

Traditionally, computers make rigid *yes* or *no* decisions, by means of decision rules based on two-valued logic: *true –false*, *yes –no*, or 1 − 0. *Fuzzy logic,* on the other hand, allows a graduation from *true* to *false*.

Many classes or *sets* have *fuzzy* rather than sharp boundaries, and this is the mathematical basis of fuzzy logic; The core of a fuzzy controller is a collection of *verbal* or *linguistic* rules of the *if–then* form. Several variables may occur in each rule, both on the *if* -side and the *then*-side.

Reflecting expert opinions, the rules can bring the reasoning used by computers closer to that of human beings[4][9].

2.11.2 Fuzzy Sets:

FL unlike Boolean logic, deals with problems that have fuzziness or vagueness. The classical set theory is based on Boolean logic, where a particular object or variable is either a member of a given set (logic I), or it is not (logic 0). On the other hand, in fuzzy set theory based on FL, a particular object has a degree of membership in a given set that may be anywhere in the range of 0 (completely not in the set) to 1 (completely in the set). For this reason, FL is often defined as multi-valued logic (0 to 1), compared to bi-valued Boolean logic. It may be mentioned that although FL deals with imprecise information, the information is processed in sound mathematical theory, which has been advanced in recent years[4][10].

Before discussing the FL theory, it should be emphasized here that basically, a FL problem can be defined as an input/output, static, nonlinear mapping problem through a "black box," as shown in Figure 2.22. All the input information is defined in the input space, it is processed in the black box, and the solution appears in the output

space. In general, mapping can be static or dynamic, and the mapping characteristics are determined by the black box's characteristics. The black box represent the fuzzy system.

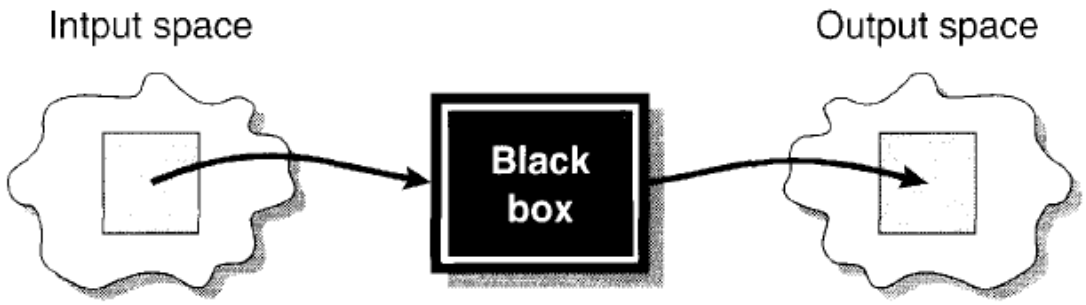

Figure 2.22 Input/output mapping problem

2.11.2.1 Membership Functions:

A fuzzy variable has values that are expressed by the natural English language. For example. The speed of a motor as a fuzzy variable can be defined by the qualifying linguistic variables Low, Mid, or High, where each is represented by a triangular or straight-line segment membership function (MF). These linguistic variables are defined as fuzzy sets or fuzzy subsets. An MF is a curve that defines how the values of a fuzzy variable in a certain region are mapped to a membership value μ (or degree of membership) between 0 and I. The fuzzy sets can have more subdivisions such as Zero, Very Low, Medium Low, Medium High. Very High.

An MF can have different shapes, as shown in Figure 2.23. The simplest and most commonly used MF is the triangular-type, which can be symmetrical or asymmetrical in shape. A trapezoidal MF (symmetrical or unsymmetrical) has the shape of a truncated triangle. Two MFs are built on the Gaussian distribution curve: a simple Gaussian curve and a two-sided composite of two different Gaussian curves. The bell MF with a flat top is somewhat different from a Gaussian function. Both the Gaussian and bell functions are smooth and non-zero at all points. A sigmoidal-type MF can be open to the right or left. Asymmetrical and closed (not open to the right or left) MFs can be synthesized using two sigmoidal functions, such as difference sigmoidal (difference between two sigmoidal functions) and product sigmoidal (product of two sigmoids). Polynomial-based curves can have several functions, including

asymmetrical polynomial curve open to the left (Polynomial-Z) and its mirror image, open to the right (Polynomial-S), and one that is zero at both ends but has a rise in the middle (Polynomial-Pi).

In addition to these types, any arbitrary MF can be generated by the user.

A singleton is a special type of MF that has a value of 1 at one point on the universe of discourse and zero elsewhere (a vertical spike). MFs can be represented by mathematical functions, segmented straight lines (for triangular and trapezoidal shapes), and look-up tables.

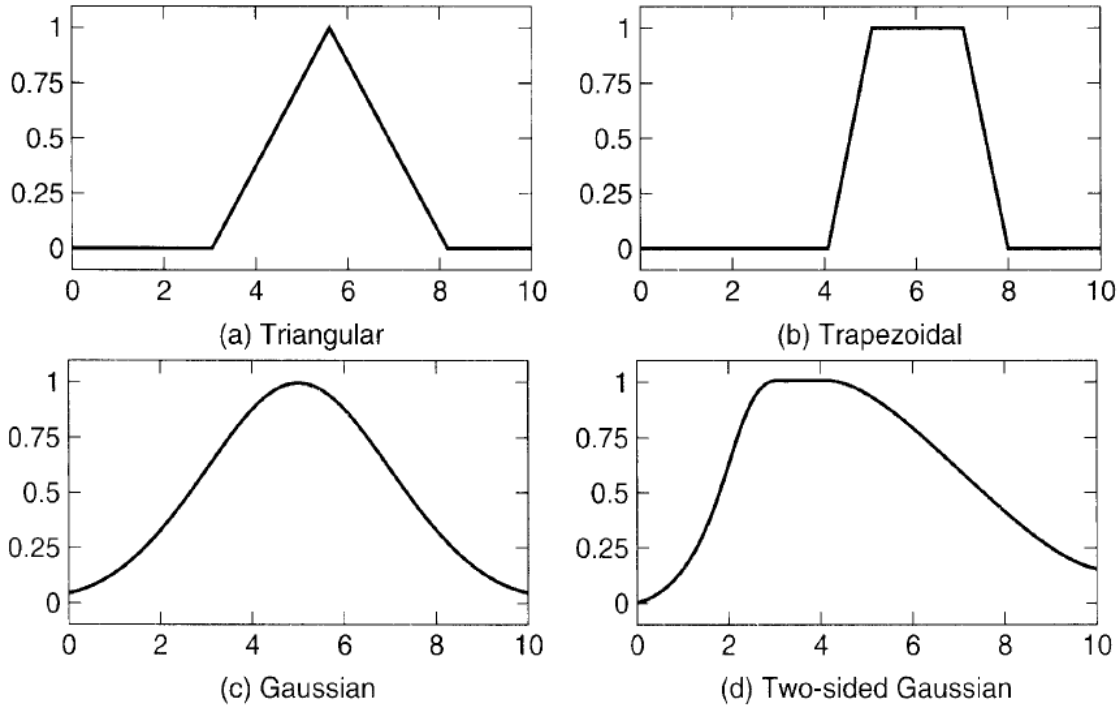

Figure 2.23: Different types of membership functions; (a) Triangular, (b) Trapezoidal,(c) Gaussian, (d) Two-sided Gaussian (Continued)

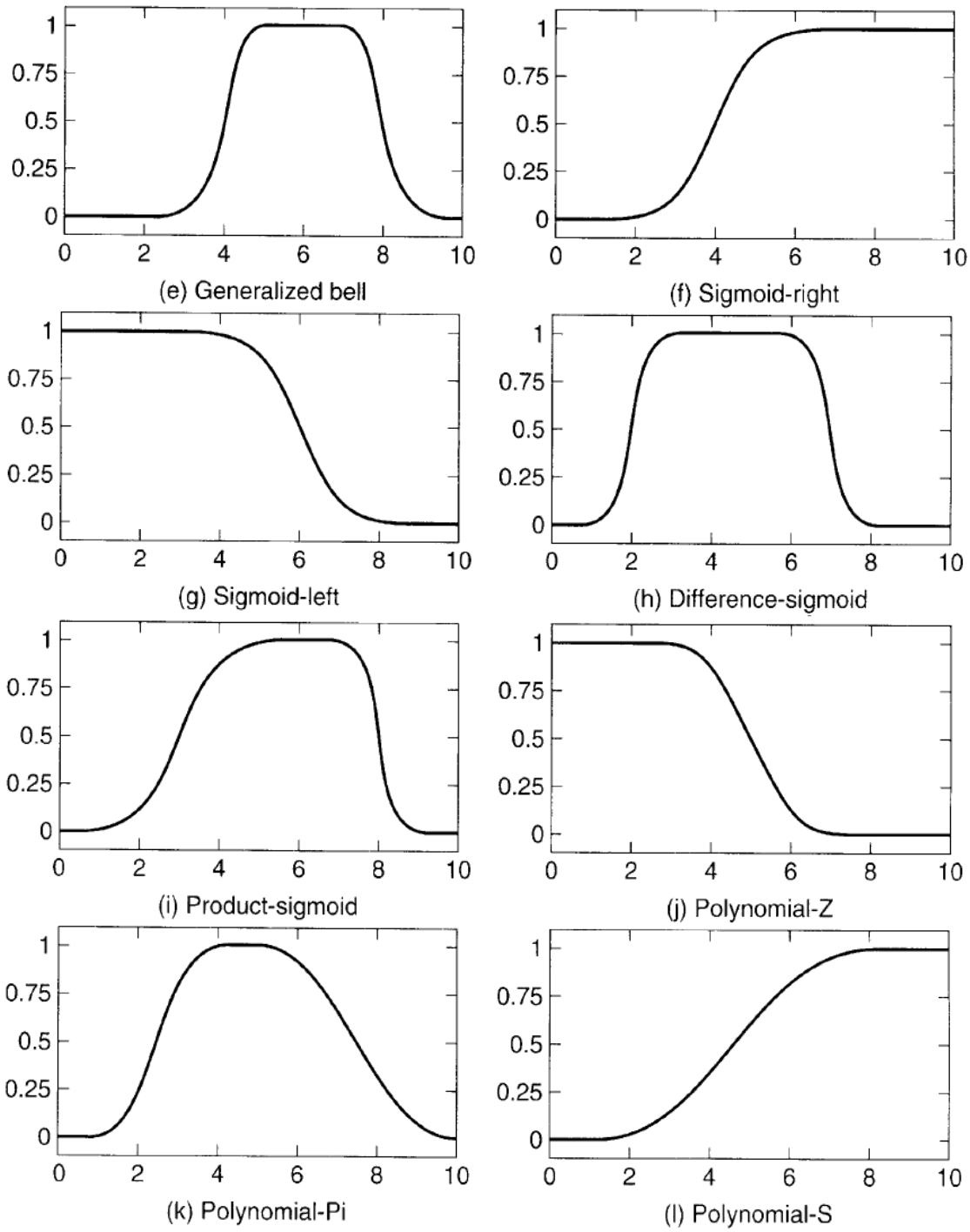

Figure 2.23: *(Cant.)* Different types of membership functions; (e) Generalized bell, (f) Sigmoid-right, (g) Sigmoid-left, (h) Difference-Sigmoid, (i) Product-Sigmoid, (j) Polynomial-Z, (k) Polynomial-Pi,
(I) Polynomial-S

2.11.2.2 Operations on Fuzzy Sets:

The basic properties of Boolean logic are also valid for FL. Figure 2.24 shows the logical operations of OR, AND, and NOT on fuzzy sets A and B using triangular MFs

and compares them with the corresponding Boolean operations on the right. Let $\mu_A(x)$, $\mu_B(x)$ denote the degree of membership of a given element x in the universe of discourse X (denoted by $X \in X$).

Union: Given two fuzzy sets A and B, defined in the universe of discourse X, the union $(A \cup B)$ is also a fuzzy set of X, with the membership function given as:

$$\mu_{A \cup B}(x) \equiv \max[\mu_A(x), \mu_B(x)] \equiv \mu_A(x) \vee \mu_B(x) \tag{2.40}$$

where the symbol "V" is a maximum operator. This is equivalent to Boolean OR logic.

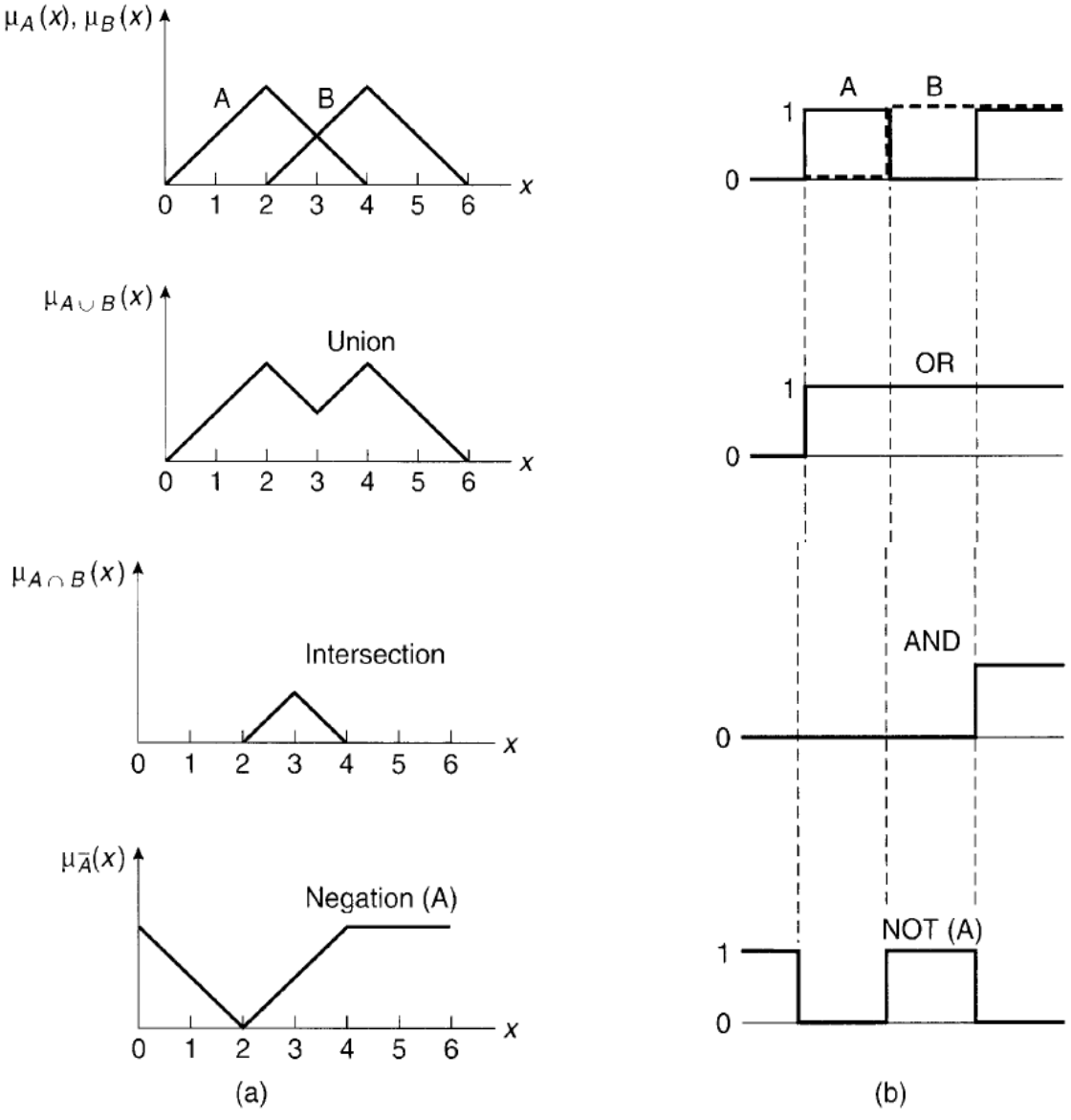

Figure 2.24 Logical operations of (a) Fuzzy sets, (b) Crisp sets

Intersection: The intersection of two fuzzy sets A and B in the universe of discourse X denoted by $A \cap B$, has the membership function given by:

$$\mu_{A\cap B}(x) \equiv \min[\mu_A(x),\mu_B(x)] \equiv \mu_A(x) \Lambda \mu_B(x) \quad (2.41)$$

where "Λ" is a minimum operator. This is equivalent to Boolean AND logic.

Complement or Negation: The complement of a given set A in the universe of discourse X is denoted by $\tilde{A}$ and has the membership function:

$$\mu_{\tilde{A}}(x) = 1 - \mu_A(x) \quad (2.42)$$

This is equivalent to the NOT operation in Boolean logic.

In FL, we can also define the following operations:

Product of two fuzzy sets: The product of two fuzzy sets A and B defined in the same universe of discourse X is a new fuzzy set, $A.B$, with an MF that equals the algebraic product of the MFs of A and B,

$$\mu_{A.B}(x) \equiv \mu_A(x).\ \mu_B(x) \quad (2.43)$$

which can be generalized to any number of fuzzy sets in the same universe of discourse.

Multiplying Fuzzy Set by a Crisp Number: The MF of fuzzy set A can be multiplied by a crisp number k to obtain a new fuzzy set called product $k.A$. Its MF is:

$$\mu_{k\,A}(x) \equiv k\ .\mu_A(x) \quad (2.44)$$

Power of a Fuzzy Set: We can raise fuzzy set A to a power m (positive real number) by raising its MF to m. The m power of A is a new fuzzy set, A^m, with MF

$$\mu_{A^m}(x) = [\mu_A(x)]^m \quad (2.45)$$

2.11.3 Fuzzy System:

A fuzzy inference system (or fuzzy system) basically consists of a formulation of the mapping from a given input set to an output set using FL, as indicated in Figure 2.22. This mapping process provides the basis from which the inference or conclusion can be made. A fuzzy inference process consists of the following five steps:

• Step1: Fuzzification of input variables

• Step 2: Application of fuzzy operator (AND, OR, NOT) in the IF (antecedent) part of the rule

• Step 3: Implication from the antecedent to the consequent (THEN part of the rule)

• Step 4: Aggregation of the consequents across the rules

• Step 5: Defuzzification

2.11.3.1 Implication Methods:

There are a number of implication methods in the literature. so we will study a few of the types that are frequently used.

2.11.3.1.1 Mamdani Type:

Mamdani, one of the pioneers in the application of FL in control systems. proposed this implication method which, is the most commonly used implication method. Let us again consider three rules in a fuzzy system, which are given in general form given as:

Rule 1: IF *X* is negative small (NS) AND *Y* is zero (ZE)

THEN Z is positive small (PS)

Rule 2: IF *X* is zero (ZE) AND *Y* is zero (ZE)

THEN Z is zero (ZE)

Rule 3: IF *X* is zero (ZE) AND *Y* is positive small (PS)

THEN Z is negative small (NS)

where X and Yare the input variables, Z is the output variable, and NS, ZE, and PS are the fuzzy sets. Figure 2.25 explains the fuzzy inference system with the Mamdani method for inputs X =-3 and Y=1.5. Note that all the rules have an AND operator. From the figure, the Degree Of Fulfillment (DOF) of Rule 1 can be given as:

$$DOF_1 = \mu_{NS}(X) \wedge \mu_{ZE}(Y) = 0.8 /\backslash\ 0.6 = 0.6 \quad (2.46)$$

where $\wedge$ =minimum operator and $\mu_{NS}(X)$ and $\mu_{ZE}(Y)$ are the MFs of X and Y, respectively. The rule output is given by the truncated MF PS', as shown in the figure. Similarly. for Rules 2 and 3. we can write

$$DOF_2 = \mu_{ZE}(X) \wedge \mu_{ZE}(Y) = 0.4 \wedge 0.6 = 0.4 \quad (2.47)$$

$$DOF_3 = \mu_{ZE}(X) \wedge \mu_{PS}(Y) = 0.4 \wedge 1.0 = 0.4 \quad (2.48)$$

The corresponding fuzzy output MFs are ZE' and NS', respectively. as indicated in the figure. The total fuzzy output is the union (OR) of all the component MFs.

$$\mu_{OUT}(Z) = \mu_{PS'}(Z) \vee \mu_{ZE'}(Z) \vee \mu_{NS'}(Z) \qquad (2.49)$$

which is shown in the lower right part of the figure.

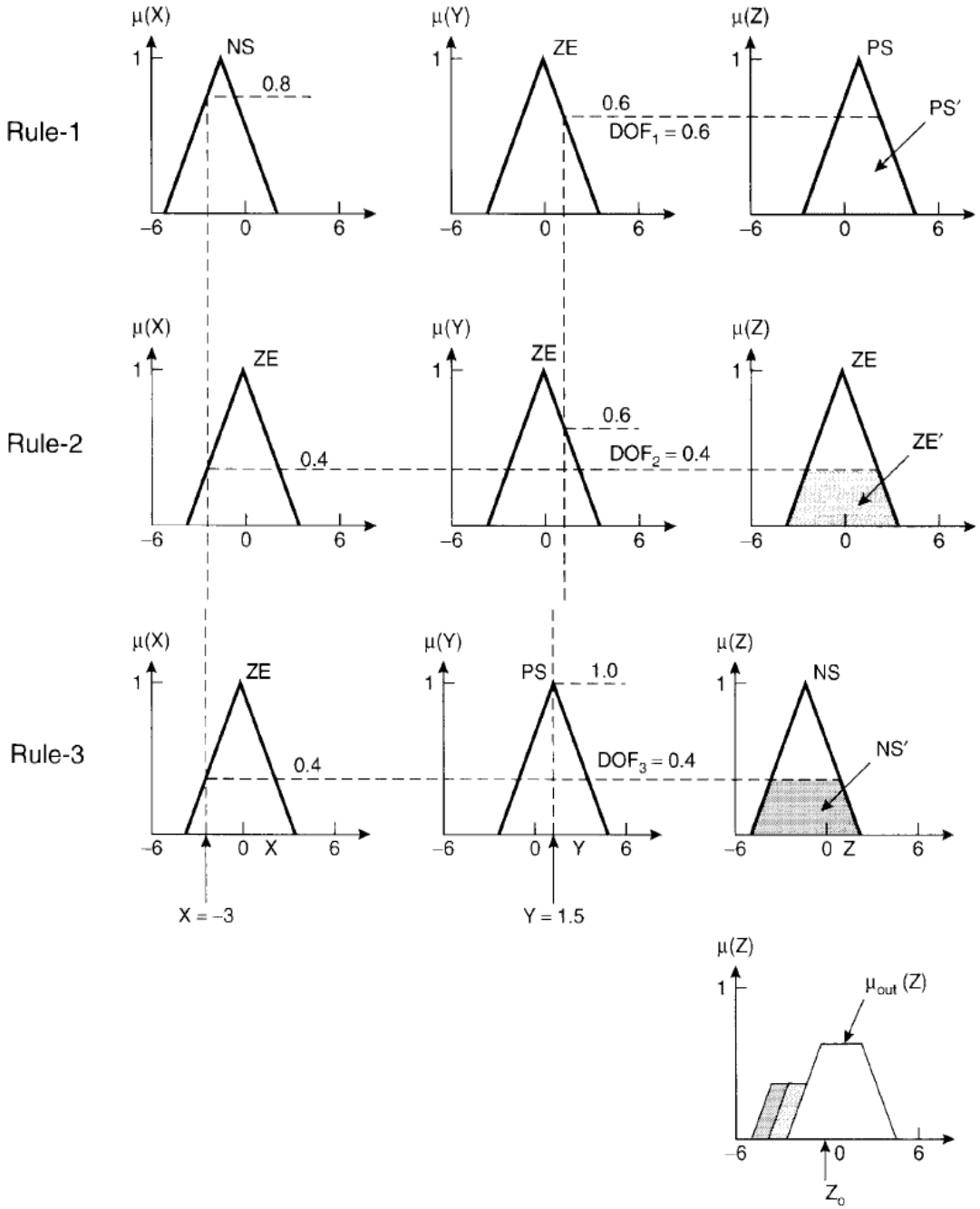

Figure 2.25: Three-rule fuzzy system using Mamdani method

2.11.3.1.2 Lusing Larson Type:

In this method, the output MF is scaled instead of being truncated, as shown in Figure 2.26. In this case, the same three rules are considered as well as the same inputs, of X =-3 and Y= 1.5 giving DOFs of DOF_1 =0.6, DOF_2 =0.4, and DOF_3 =0.4. The output MF PS of Rule 1 is scaled so that the output is PS' with a peak value of 0.6 as shown. Similarly, Rules 2 and 3 give output MFs ZE' and NS', each with a peak value of 0.4 as indicated. The total output MF is given by Equation (2.49). The output area is somewhat different from that of the Mamdani method, and the corresponding crisp output will differ slightly.

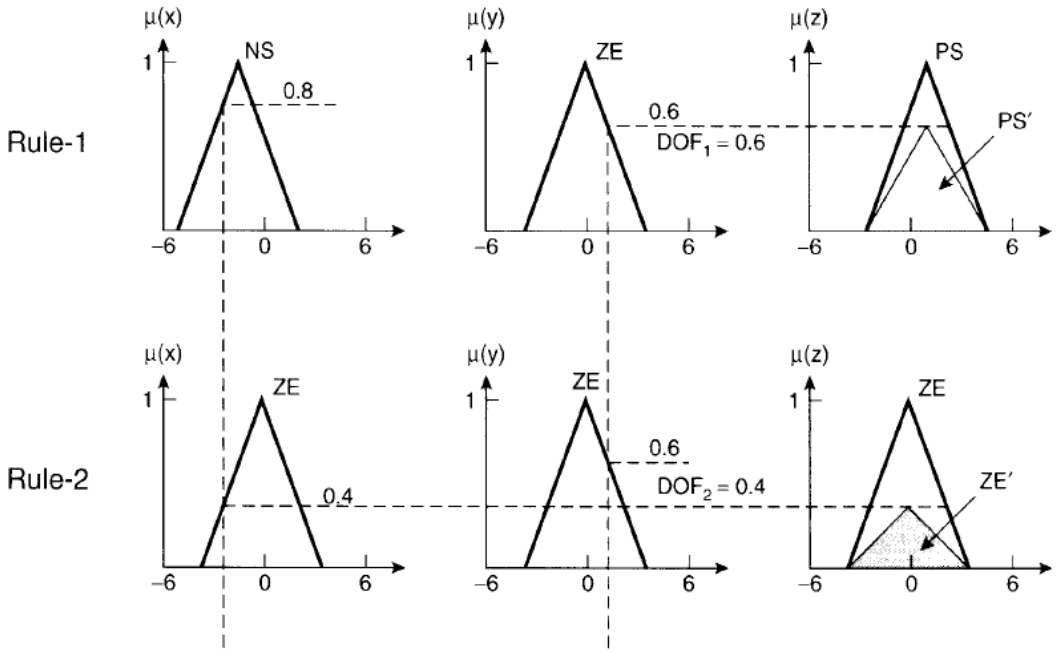

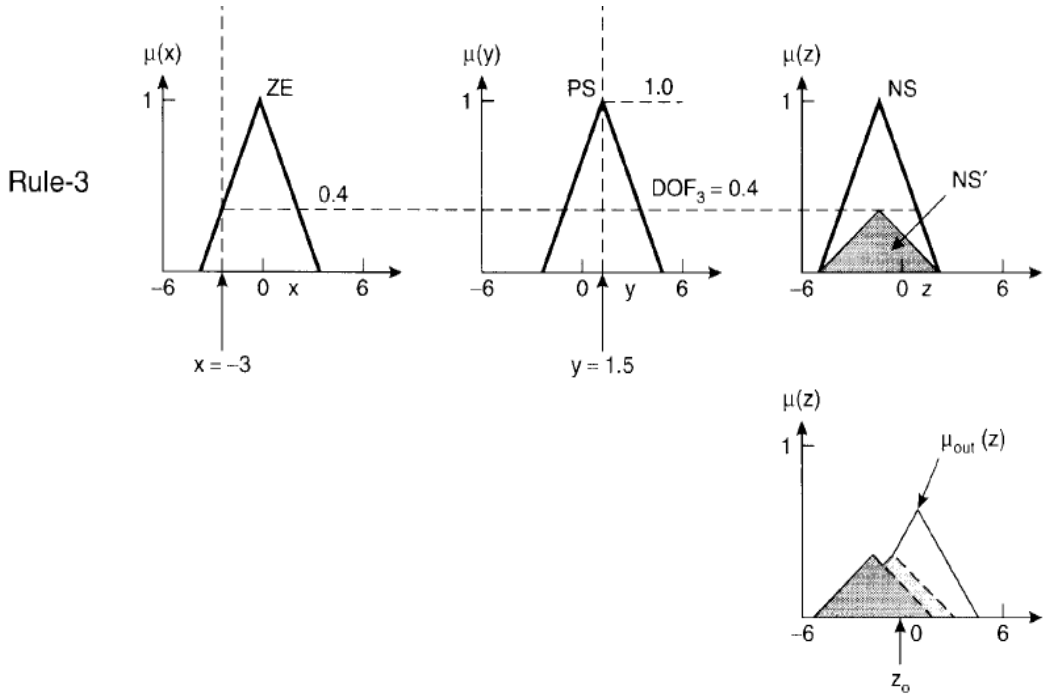

Figure 2.26 Three-rule fuzzy system using Lusing Larson method

2.11.3.1.3 Sugeno Type:

The Sugeno, or Takagi-Sugeno-Kang method of implication was first introduced in 1985. The difference here is that unlike the Mamdani and Lusing Larson methods, the output MFs are only constants or have linear relations with the inputs. With a constant output MF (singleton), it is defined as the zero-order Sugeno method, whereas with a linear relation, it is known as the first-order Sugeno method.

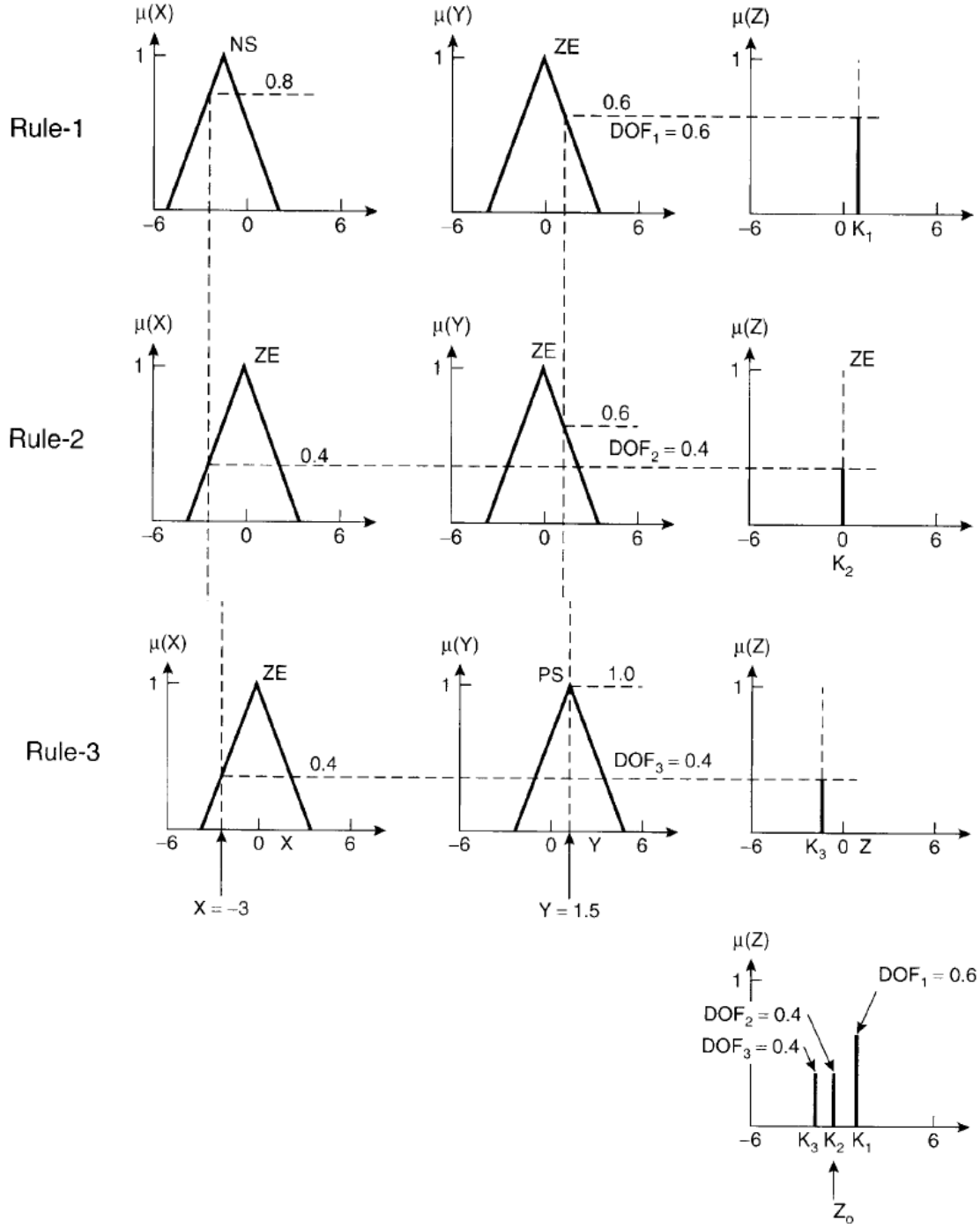

Figure 2.27 Three-rule fuzzy system using Sugeno (zero-order) method

Figure 2.27 shows a three-rule fuzzy system using the Sugeno zero-order method where the rules read as:

Rule 1: IF *X* is NS AND *Y* is ZE THEN $Z=K_1$

Rule 2: IF *X* is ZE AND *Y*is ZE THEN $Z= K_2$

Rule 3: IF *X* is ZE AND *Y*is PS THEN $Z= K_3$

The constants K_1, K_2, and K_3 are crisply defined constants, as shown in the figure in the consequent part of each rule. The output MF in each rule is a singleton spike, which is multiplied by the respective DOF to contribute to the fuzzy output of each rule. These MFs (truncated vertical segments) are then aggregated to constitute the total fuzzy output as shown in the figure. Fortunately, it can be shown that if the Mamdani, Lusing Larson, and Sugeno methods are applied to the same problem, the output will be approximately the same.

2.11.3.2 Defuzzification Methods:

So far, we have discussed the different steps of a fuzzy inference system. The result of the implication and aggregation steps is the fuzzy output, which is the union of all the outputs of individual rules that are validated or "fired." Conversion of this fuzzy output to crisp output is defined as defuzzification. We will now discuss a few important methods of defuzzification.

2.11.3.2.1 Center of Area (COA) Method:

In the COA method (often called the center of gravity method) of defuzzification, the crisp output Z_o of the Z variable is taken to be the geometric center of the output fuzzy value $\mu_{OUT}(Z)$ area, where $\mu_{OUT}(Z)$ is formed by taking the union of all the contributions (see, for example, the lower right part of Figure (2.25)). The general expression for COA defuzzification is:

$$Z_o = \frac{\int Z.\mu_{OUT}(Z)dZ}{\int \mu_{OUT}(Z)dZ} \qquad (2.50)$$

With a discretized universe of discourse, the expression is:

$$Z_o = \frac{\sum_{i=1}^{n} Z_i \mu_{OUT}(Z_i)}{\sum_{i=1}^{n} \mu_{OUT}(Z_i)} \qquad (2.51)$$

2.11.3.2.2 Height Method:

In the height method of defuzzification, the COA method is simplified to consider only the height of each contributing MF at the mid-point of the base.

2.11.3.2.3 Mean of Maxima (MOM) Method:

The height method of defuzzification is further simplified in the MOM method, where only the highest membership function component in the output is considered.

$$Z_O = \sum_{m=1}^{M} \frac{Z_m}{M} \tag{2.52}$$

where Z_m = *mth* element in the universe of discourse, where the output MF is at the maximum value, and M =number of such elements.

2.11.3.2.4 Sugeno Method:

In the Sugeno method, defuzzification is very simple. For example, In the zero-order method shown in Figure 2.27, the defuzzification formula is :

$$Z_O = \frac{K_1.DOF_1 + K_2.DOF_2 + K_3.DOF_3}{DOF_1 + DOF_2 + DOF_3} \tag{11.25}$$

2.11.4 Fuzzy Control:

2.11.4.1 Why Fuzzy Control?

The control algorithm of a process that is based on FL or a fuzzy inference system, as discussed above, is defined as a fuzzy control. In general, a control system based on Artificial Intelligent (AI) is defined as intelligent control. A fuzzy control system essentially embeds the experience and intuition of a human plant operator, and sometimes those of a designer and/or researcher of a plant. The design of a conventional control system is normally based on the mathematical model of a plant. If an accurate mathematical model is available with known parameters, it can be analyzed, for example, by a Bode or Nyquist plot, and a controller can be designed for the specified performance. Unfortunately, for complex processes, such as cement plants, nuclear reactors, and the like, a reasonably good mathematical model is difficult to find. On the other hand, the plant operator may have good experience for controlling the process. Power electronics system models are often ill-defined. Even if a plant model is well-known, there may be parameter variation problems. Sometimes, the model is multivariable, complex, and nonlinear, such as the dynamic *d-q* model of

an ac machine. Vector or field-oriented control of a drive can overcome this problem, but accurate vector control is nearly impossible, and there may be a wide parameter variation problem in the system. Fuzzy control, on the other hand, does not strictly need any mathematical model of the plant. It is based on plant operator experience and heuristics, as mentioned previously, and it is very easy to apply. Fuzzy control is basically an adaptive and nonlinear control, which gives robust performance for a linear or nonlinear plant with parameter variation.

2.11.4.2 Control Principle:

The general structure of a fuzzy feedback control system is shown in Figure 2.28. The loop error *E* and change in error *CE* signals are converted to the respective per unit signals *e* and *ce* by dividing by the respective base factors, that is, $e = E/GE$ and $ce = CE/GC$. Similarly, the output plant control signal *U* is derived by multiplying the per unit output by the scale factor *GU,* that is, $DU = du.GU$, and then summed to generate the *U* signal.

The advantage of fuzzy control in terms of per unit variables is that the same control algorithm can be applied to all the plants of the same family. Besides, it becomes convenient to design the fuzzy controller. The scale factors can be constant or programmable. The processes of fuzzification, evaluation of control rules from the rule base and database (defined as the knowledge base), and defuzzification has already been discussed.

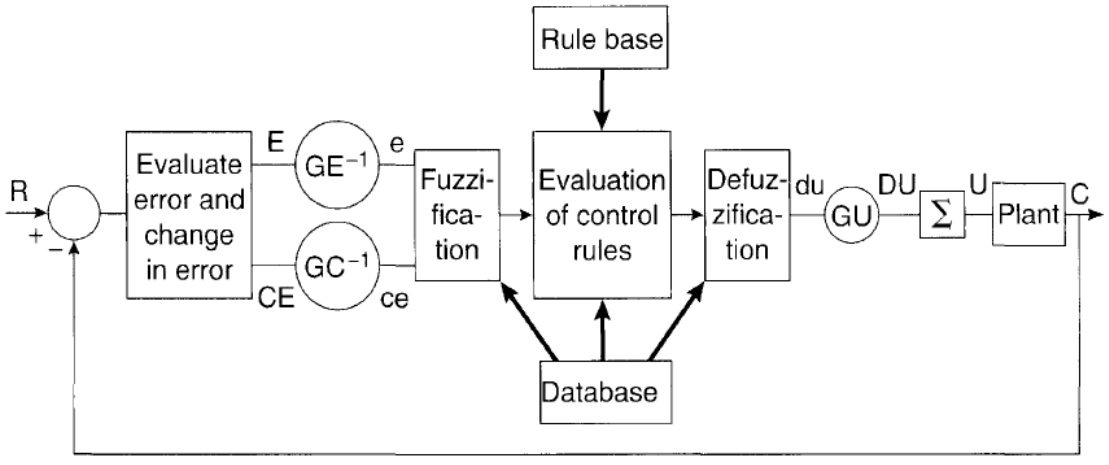

Figure 2.28: Structure of fuzzy control in feedback system

2.11.5 Fuzzy Logic Toolbox:

In this section, we will introduce a commonly used fuzzy system development tool. The Fuzzy Logic Tool box (Math Works. Inc.) [3] is a user-friendly fuzzy program development tool in the MATLAB environment. Development can be done using either Graphical User Interface (GUI) or command-line functions. The toolbox also includes fuzzy clustering and an adaptive neuro-fuzzy inference system (ANFIS) technique. Once a fuzzy program is developed, its performance can be tested by embedding it in the SIMULINK simulation of the system for fine-tuning. And then, the final stand-alone C program (with the fuzzy inference engine) can be generated, compiled, and downloaded to a DSP for real-time implementation. Or else, the program can be embedded in other external applications.

There are five primary graphical tools for building, editing, and observing fuzzy inference systems in the Fuzzy Logic Toolbox. They are:

- Fuzzy Inference System (FIS) Editor
- Membership Function (MF) Editor
- Rule Editor
- Rule Viewer
- Surface Viewer

2.11.5.1 FIS Editor:

The FIS Editor, as shown in Figure 2.29, displays general information about a fuzzy system. At the top left, the names of the defined input fuzzy variables are indicated, and at the right, the output variables are shown. The MFs shown in the boxes are simple icons and do not indicate the actual MFs. Below this, the system name and inference method (either Mamdani or Sugeno) are indicated. At the lower left, the various steps of the inference process, which are user-selectable, are shown. At the lower right, the name of the input or output variable, its associated MF type, and its range are displayed.

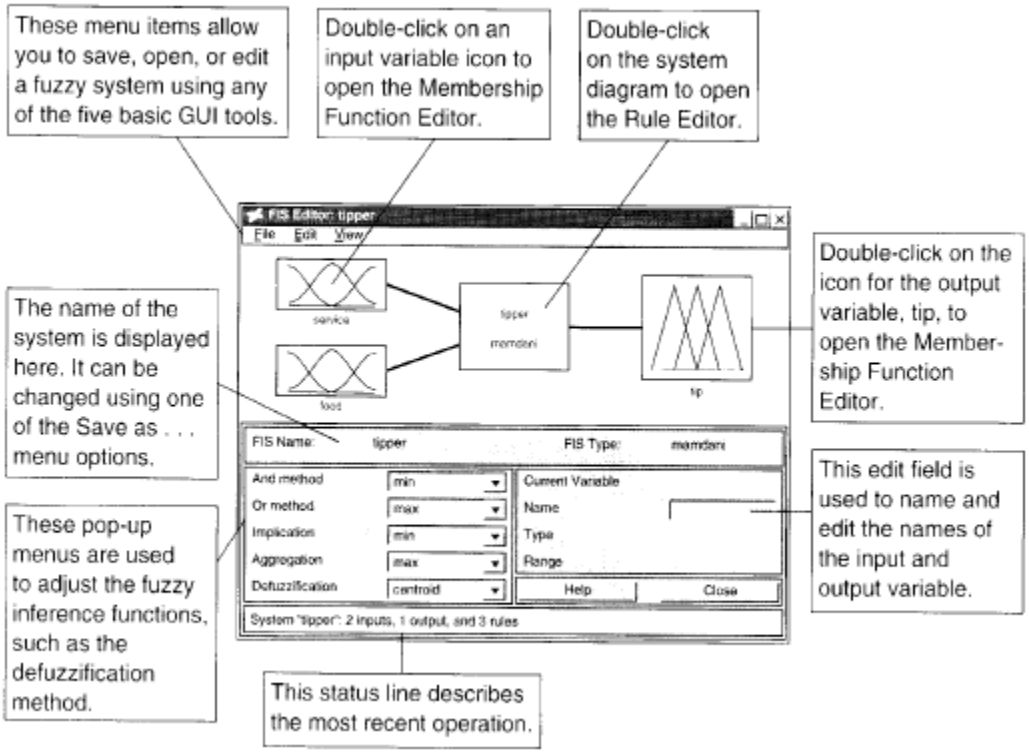

Figure 2.29 user interface for FIS Editer

2.11.5.2 Membership Function Editor:

The MF Editor displays and permits editing of all the MFs associated with the input and output variables. Figure 2.30 shows the user interface of the MF Editor. At the upper left, the FIS variables whose MFs can be set are shown. Each setting includes a selection of the MF type and the number of MFs of each variable. At the lower right, there are controls that permit you to change the name, type, and parameters (shape) of each MF. Once you have selected it, the MFs of the current variable, which are being edited, are displayed in the graph. At lower left, information about the current variable is given. In the text field, the range (universe of discourse) and display range of the current plot of the variable under consideration can be changed.

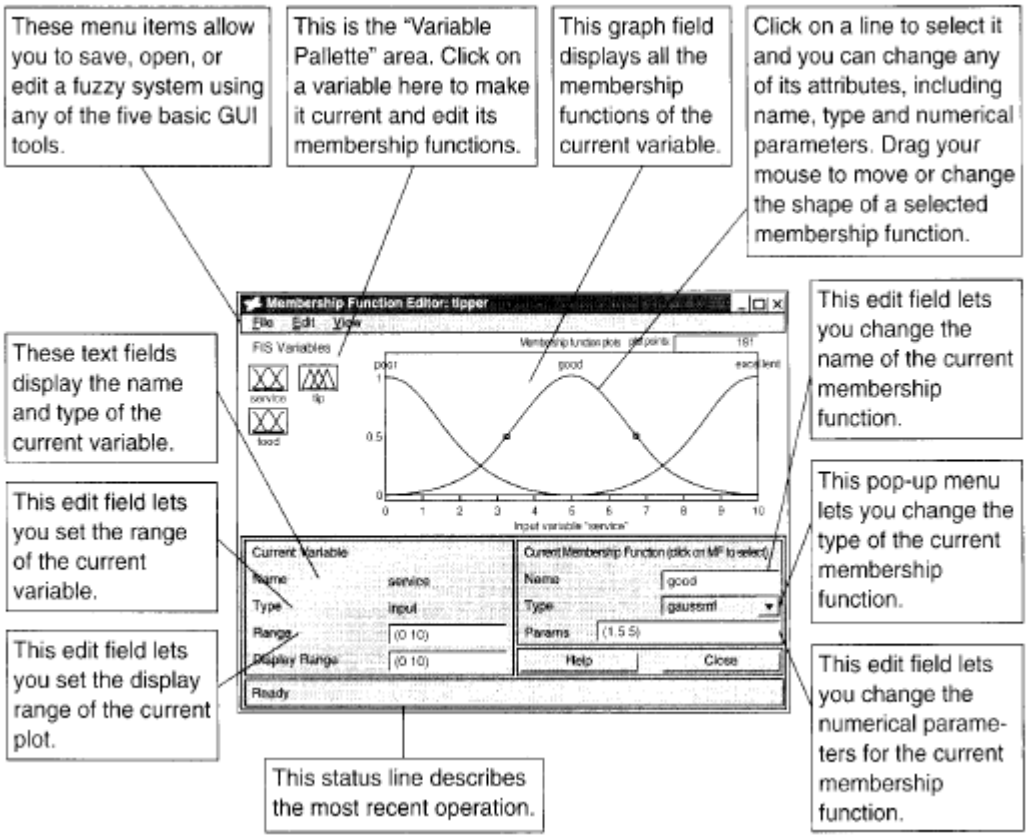

Figure 2.30: user interface for MF Editer

2.11.5.3 Rule Editor:

Once the rule matrix is designed on paper and the fuzzy variables are defined in the FIS Editor, construction of the actual rules by the Rule Editor is fairly easy, as shown in Figure 2.31. The logical connectives of rules, AND, OR, and NOT can be selected by buttons. The rules can be changed, deleted, or added, as desired.

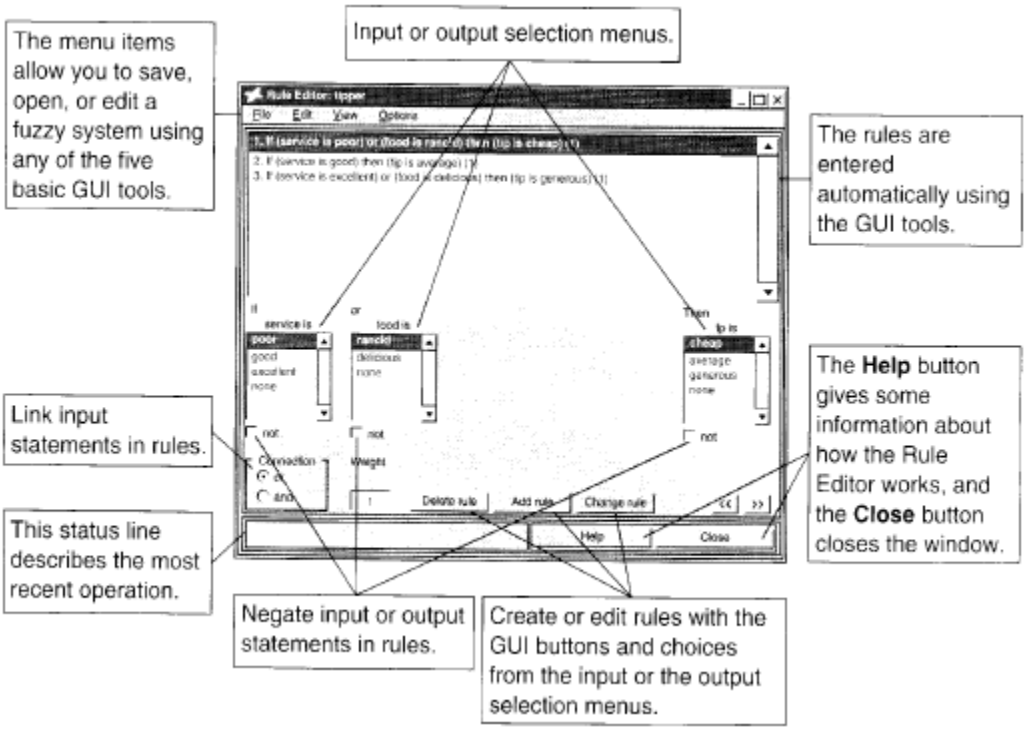

Figure 2.31: user interface for Rule Editer

2.11.5.4 Rule Viewer:

Once the fuzzy algorithm has been developed, the Rule Viewer, as shown in Figure 2.32, essentially gives a micro view of the FIS, where the operation and contribution of each rule is explained in detail. Each rule is a row of plots, and each column is a variable. For a certain setting of the input variables, the output contribution of each rule, the total fuzzy output, and the corresponding defuzzified output are shown. The Rule Viewer with its roadmap of operation of the whole fuzzy algorithm, permits fine-tuning of the MFs and rules.

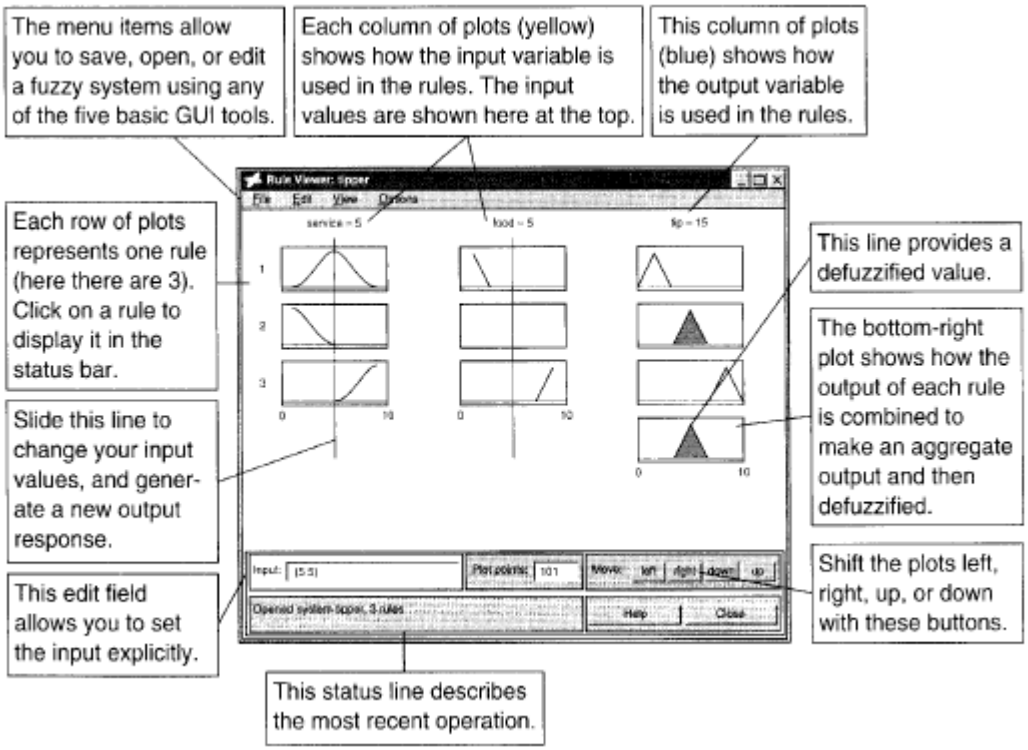

Figure 2.32: user interface for Rule Viewer

2.11.5.5 Surface Viewer:

After the fuzzy algorithm has been developed, the Surface Viewer permits you to view the mapping relations between the input variables and output variables, as shown in Figure 2.33. The plot may be three-dimensional, as shown, or two-dimensional. For a larger number of input/output variables, the variables for the Surface Viewer can be selected. Again, by closely examining the Surface Viewer, the algorithm can be iterated.

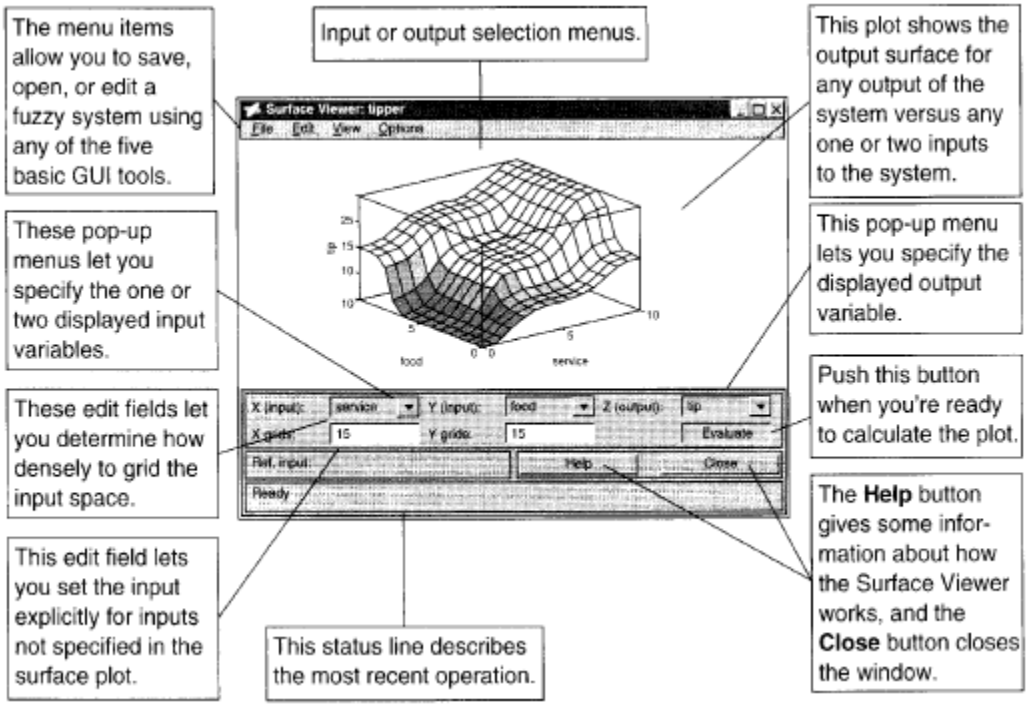

Figure 2.33 user interface to control Surface Viewer

2.12 Summary of The Chapter:

Induction motors, especially those of the squirrel-cage type, are the most common sources of mechanical power in industry. Supplied from a three phase ac line, they are simple, robust, and inexpensive. Although most motors operate with a fixed frequency resulting in an almost constant speed, ASDs are increasingly introduced in a variety of applications. Such a drive must include a power electronic converter to control the magnitude and frequency of the voltage and current supplied to the motor. A control system governing the operation of the drive system is usually of the digital type.

Common mechanical loads can be classified with respect to their inertia, to the torque-speed characteristic (mechanical characteristic), and to the control requirements. Depending on the particular application, the driving motor may operate in a single quadrant, two quadrants, or four quadrants of the (ω_M ,T_M) plane.

Scalar control methods, in which only the magnitude and frequency of the fundamental voltage and current supplied to the motor are adjusted, are employed in low-performance drives. If high dynamic performance of a drive is required under

both the steady-state and transient operating conditions, vector techniques are used to adjust the instantaneous values of voltage and current.

Operation of the induction motor is based on the ingenious principle of induction of EMFs and currents in the rotor that is not directly connected to any supply source. Three-phase currents in stator windings produce a revolving magnetic field, whose angular velocity, called a synchronous velocity of the motor, is proportional to the supply frequency and inversely proportional to the number of pole pairs. The latter parameter, an integer, depends on the configuration of the windings, and it determines the field pattern. The rotor rotates with a speed different than that of the field.

Consequently, lines of magnetic flux intersect rotor conductors, inducing the EMFs and currents. Slip, *s,* which is the relative difference of speeds of the field and rotor, is one of the most important quantities defining operating conditions of an induction machine.

Analysis of the steady-state operation of the induction motor is based on the per-phase equivalent circuit. The mechanical load of the motor is modeled by the equivalent load resistance. The developed torque resulting from interaction between the field and rotor currents strongly depends on the slip. It can be calculated as a ratio of power dissipated in equivalent load resistances of all three phases of the motor to the angular velocity of the rotor. The torque reaches a maximum value, the pull-out torque, at a speed lower than rated. The pull-out torque and the starting torque are higher than the rated torque. Other steady-state characteristics, such as the stator current versus speed, can also be determined from the equivalent circuit. Fuzzy set theory based on FL, a particular object has a degree of membership in a given set that may be anywhere in the range of 0 to 1. A fuzzy inference system basically consists of a formulation of the mapping from a given input set to an output set using FL. Fuzzy control does not strictly need any mathematical model of the plant. It is based on plant operator experience and heuristics. The Fuzzy Logic Toolbox is a user-friendly fuzzy program development tool in the MATLAB environment.